

XPS and Carbon-13 NMR Spectroscopic Analysis
of Composite Rocket Propellants,

by

Elroy Wayne, \\Kauffman,,II

Thesis submitted to the Graduate Faculty of the Virginia
Polytechnic Institute and State University in partial fulfillment of
the requirements for the degree of

MASTER OF SCIENCE

in

Chemistry

APPROVED:

H. M. Bell, Chairman

J. P. Wightman

T. C. Ward

February, 1983
Blacksburg, Virginia

TO MY PARENTS

Acknowledgments

I, hereby, express my gratitude toward my research advisor, Dr. H. M. Bell, for his ideas, encouragement and help in this research. I would also like to thank Dr. J. P. Wightman and Dr. T. C. Ward for their valuable consultations.

Special thanks to _____ who valiantly tried to keep the ESCA operational.

The financial support from the U.S. Army Missile Command is appreciated.

Table of Contents

	<u>Page</u>
Acknowledgments.....	iii
List of Tables.....	vi
List of Figures.....	vii
General Introduction.....	1
Historical.....	5
Part I: Carbon-13 NMR.....	11
Introduction.....	11
Experimental.....	13
Results and Discussion.....	16
Source of Carbon-13 Spectrum.....	16
Vinyllic Content Analysis.....	23
Summary.....	32
Part II: Photoelectron Spectroscopy.....	33
Introduction.....	33
Experimental.....	34
Results and Discussion.....	35
X-Ray Degradation of AP.....	39
SEM of Propellant Surface.....	39
Spectral Analysis of N(1s) Photopeak.....	52
Spectral Analysis of Cl(2p) Photopeak.....	63
Summary.....	72

	<u>Page</u>
References.....	73
Vita.....	76
Abstract.....	

List of Tables

<u>Table</u>	<u>Page</u>
I. Composition of Propellant Reference Mixtures.....	15
II. Comparison of Carbon-13 Peak Positions.....	29
III. Vinylic Character of the Propellant.....	31

List of Figures

<u>Figure</u>	<u>Page</u>
1. Proton NMR Spectrum of HTPB.....	17
2. Carbon-13 NMR Spectrum of HTPB.....	18
3. Saturated Carbon Region of HTPB.....	20
4. Unsaturated Carbon Region of HTPB.....	21
5. Carbon-13 Spectrum of Propellant Aged at 190°F for 24 months.....	22
6. Carbon-13 Spectrum of Extractables from the 190°F Propellant.....	24
7. Carbon-13 Spectrum of Reswelled Propellant (190°F)..	25
8. Carbon-13 Spectrum of Propellant Aged at 75°F for 24 months.....	26
9. Carbon-13 Spectrum of Propellant Aged at 110°F for 24 months.....	27
10. Carbon-13 Spectrum of Propellant Aged at 150°F for 24 months.....	28
11. XPS Cl(2p) Spectrum of AP.....	36
12. XPS N(1s) Spectrum of AP.....	37
13. XPS Cl(2p) Spectrum of NH ₄ Cl.....	38
14. XPS N(1s) Spectrum of HTPB.....	40
15. XPS Widescan Spectrum of Propellant Aged at 75°F for 24 months.....	41
16. XPS O(1s) Spectrum of Propellant Aged at 75°F for 24 months.....	42
17. XPS C(1s) Spectrum of Propellant Aged at 75°F for 24 months.....	43
18. XPS Degradation of Perchlorate in AP.....	44

	<u>Page</u>
19. XPS Degradation of Perchlorate in Mix A.....	45
20. XPS Degradation of Perchlorate in Mix 1.....	46
21. XPS Degradation of Perchlorate in Mix 2.....	47
22. XPS Degradation of Perchlorate in HTPB-AP.....	48
23. Change in Perchlorate Concentrations under XPS Conditions.....	49
24. SEM of Unaged Propellant (170X).....	50
25. SEM of Changed Propellant (850X).....	51
26. XPS Degradation of N(1s) in Aged Propellant.....	53
27. Change in N(1s) Source for Mix 1.....	55
28. Change in N(1s) Source for Mix 2.....	56
29. Change in N(1s) Source for Sample VIII.....	57
30. Change in N(1s) Source for Sample VII.....	58
31. Change in N(1s) Source for Mix A.....	59
32. Change in N(1s) Source for Mix 3.....	60
33. Change in N(1s) Source for Samples Aged at HT&% Overtime.....	61
34. Change in N(1s) Source for Sample Aged at LT&% Overtime.....	62
35. Cl ⁻ Concentration Changes Between Ageing Conditions for Sample VII.....	64
36. Cl ⁻ Concentration Changes Between Ageing Conditions for Sample VIII.....	65
37. Cl ⁻ Concentration Changes Between Ageing Conditions for Mix 1.....	66
38. Cl ⁻ Concentration Changes Between Propellant Ageing Conditions.....	67

	<u>Page</u>
39. Cl ⁻ Concentration Changes Between Propellant Longterm Ageing Conditions.....	68
40. Cl ⁻ Concentration Changes Between Mix A Ageing Conditions.....	69
41. Cl ⁻ Concentration Changes Between Mix 2 Ageing Conditions.....	70
42. Longterm Cl ⁻ Concentration Changes in Samples.....	71

General Introduction

The purpose of this research was to investigate the suitability of Carbon-13 Fourier Transform Nuclear Magnetic Resonance Spectroscopy and X-ray Photoelectron Spectroscopy to the detection and quantification of degradation processes in an ammonium perchlorate(AP)/hydroxy-terminated polybutadiene (HTPB) composite solid propellant system. A solid composite propellant consists of an inorganic oxidizer (generally ammonium perchlorate), a fuel (aluminum), and a binder (organic polymers). A propellant is prepared by mixing powdered AP and aluminum with (uncured) binder, such as low molecular weight HTPB. The binder is then "cured" by adding a difunctional isocyanate and placed into a hot environment until urethane linkages are formed. If crosslinking is desired a small amount of trifunctional isocyanate is also used. When the propellant is ignited it releases low molecular weight gases in a controlled manner such that they can be directed through an exhaust nozzle of a rocket motor to provide propulsion for a rocket.

The first composite propellant, gunpowder, was developed by the Chinese centuries ago. Modern composite propellants first appeared in 1945 when a crystalline oxidizer and a metal powder additive were bound into an inhomogeneous solution by a binder which provides the propellant with the desired mechanical properties. Due to the heterogeneity of a composite propellant, the size and dispersion of the particles in the binder affects the performance of the propellant.

Previous work in composite propellant systems has concentrated on

the relationship between the age of the propellant and the decline in its performance and/or mechanical properties. Ageing studies on these relationships have been carried out in two ways: 1) by normal ageing, or 2) by accelerated ageing. Accelerated ageing at elevated temperatures is done to compress the time scale so that extrapolations can be made back to a normally aged propellant. However, these back extrapolations sometimes do not match the actual conditions which are observed. An objective of an ageing study is to predict or determine the "failure" point at which the performance or mechanical characteristics of the propellant will lead to rocket motor failure. Another objective of the ageing study is the establishment of the ageing mechanism. Once the decomposition mechanism is known steps can be taken to increase the life of the propellant.

Previous analytical work on solid propellants has concentrated on correlating the age of a propellant with changes in its mechanical properties. Many studies have measured changes in the tensile strength of the propellant as a function of its age. Other analyses have used the methods of Differential Scanning Calorimetry (DSC) and Thermogravimetry (TG) to follow the decomposition of a propellant. Studies have also used IR and Internal Reflectance IR to follow the ageing process. Of these methods only IR directly yields information on chemical changes which occur during the ageing process.

Carbon-13 NMR allows one to directly observe the carbon backbone of a molecule. Since the natural abundance of ^{13}C is only 1% and since it has a small magnetic moment, the overall sensitivity of ^{13}C is about

1/6000th of the ^1H . However the use of Fourier Transform instrumentation in conjunction with the blanket decoupling of protons yields spectra whose signal-to-noise ratio is comparable to that of proton NMR spectra. A major advantage of this method that the large chemical shift range allows the spectrum to be so spread out that the chemical shifts of the carbons rarely overlap. However, in polymers this high resolution can be significantly lowered due to line broadening.

X-ray Photoelectron Spectroscopy (XPS), commonly called ESCA (for electron spectroscopy for chemical analysis), utilizes a source of ionizing radiation, x-rays, to eject electrons from a sample. The kinetic energy of the ejected photoelectron is given by

$$E_p = h\nu - E_b$$

where E_p is the kinetic energy of the photoelectron, $h\nu$ is the energy of the incident photon, and E_b is the binding energy of the electron in its particular shell. ESCA permits the direct probing of the valence and core electrons, where much chemical information is contained. A photoelectron spectrum is characteristic of the material from which it comes. Since the positions of photoelectron lines can be determined from these spectra, and the photoelectron energies are characteristic of the atomic levels of a given element, these energies can be used as the basis for elemental identification. Due to the fact that the escape depth of the photoejected electrons is limited to about the first 50Å of a sample surface, this technique has been used for surface

analysis. This can be viewed as advantageous for the present study in that the propellant degradative process occurs at the HTPB/AP interface.

Historical

Investigations into the decomposition processes in composite propellants take several approaches, some just study the oxidizer, while a few look at the binder. A majority of the studies use simulated or real propellant mixtures for their samples. These studies age the propellants at "low" temperatures or at relatively high temperatures for various lengths of time.

Verneker, Kishore, and Mohan⁽¹⁾ attempted to correlate the rate of thermal decomposition of a propellant and the oxidizer to the propellant burning rate. They found that not only was the burning rate of the propellant related to the thermal decomposition of the propellant, but it is also related to the thermal decomposition of its oxidizer, ammonium perchlorate. Their earlier work had previously shown that ammonium perchlorate decomposition plays a significant role in the propellant decomposition, and that condensed phase reactions are important in the combustion of the propellant.⁽²⁾

Verneker, Kishore, and Prasad⁽³⁾ studied ageing behavior, leading to ballistic changes, as a function of oxidizer loading in polystyrene (PS)/ammonium perchlorate (AP) solid propellants. The ageing studies were carried out at 100°C in air. They found that the thermal decomposition rates at both 230 and 260°C decreased as the oxidizer loading in the propellants increased from 75 to 80%. The results lead them to the conclusion that the thermal decomposition of the propellant may be responsible for bringing about the ballistic changes during the

ageing process. IR studies of the binder portion of the aged propellant indicated that peroxide formation occurs during the course of ageing and that peroxide formation for a particular storage time and temperature increases as the loading decreases. Finally they confirmed their earlier results that a propellant with a higher oxidizer loading ages more slowly than a propellant with a lower loading.

Various transition metal compounds are known which increase the burning range of an AP-oxidized composite propellant. The more dispersed the catalyst is in a propellant the higher the burn rate. Jacobs and Russell-Jones^(4,5) clarified the sublimation and decomposition mechanism of AP. They favor an initial proton transfer from NH_4^+ to ClO_4^- to generate HClO_4 and NH_3 , which during combustion desorb from the surface into the gas phase. Pittman⁽⁶⁾ and Pearson^(7,8) suggest that catalysts act by catalyzing the decomposition of HClO_4 , or its immediate decomposition products, in the gas phase. Osada⁽⁹⁾ indicated that HClO_4 was effective in accelerating the rate of AP thermal decomposition and that the catalysis occurs in the gas phase, not in the solid phase.

Dauerman, Kimmel, and Wu⁽¹⁰⁾ used Internal Reflectance Spectroscopy to study the IR spectra of AP crystal surfaces being heated up to 250°C . Good results were not obtained due to the inability to resolve significant bands because of the inherent limitations of this type of spectroscopy. They observed no new Cl-O-N species and assume that any NH_3 and HClO_4 which was formed went into the gas phase and was not observed. The lack of observable

intermediary states probably indicates that the transformation of the intermediate state to gaseous products is too rapid to be observed.

Verneker, Rajalekshmi, and Jain⁽¹¹⁾ studied the thermal decomposition of an AP based solid composite propellant using carboxyl terminated polybutadiene (CTPB) as a binder employing the techniques of TG and DTA. They found that the thermal decomposition characteristics of the propellant were quite similar to those of pure AP with similar activation energies. They found that the topo-chemical behavior of the propellant in the form of a block is a rare classical example of solid state decomposition similar to the well known (Garner, 1955) examples of LiAlH_4 , mercury fulminate and potassium azide viz. (i) an initial reaction occurring on the surface of the crystals; (ii) formation of nuclei of a new phase, and (iii) a reaction occurring at the interface between the two phases. In 1968, Verneker and Maycock showed that AP also behaves in a similar fashion.

Schedlbauer,⁽¹²⁾ Myers,⁽¹³⁾ and Layton⁽¹⁴⁾ studied the mechanism of ageing of CTPB, HTPB, and PBAN-based propellants. All of them observed that the propellant becomes hard during ageing from an increase in the extent of crosslinking. The crosslinking in these polymers can occur via reactive groups or through the double bonds in the polymer backbone. Experiments were conducted to distinguish between the two processes. It was concluded that the crosslinking during ageing occurs through the interlacing of double bonds, which involves oxidative attack by the HClO_4 formed during AP decomposition.

From accelerated ageing studies in the temperature range 40-75°C

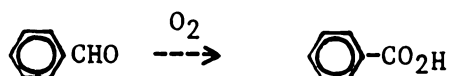
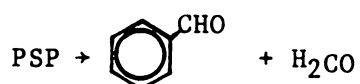
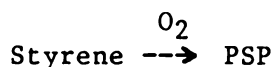
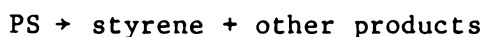
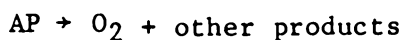
of five cast composite propellants, Kuletz and Pakulak⁽¹⁵⁾ have shown that the primary component altered at the exposed surface is the binder, whereas in the interior it is the oxidizer. However, they found that the activation energies for surface, subsurface and bulk material to be very similar. Schedlbauer⁽¹²⁾ observed that polyurethane and CTPB-based propellants harden during ageing, which he attributed to cross-linkage through the double bonds present in the main chain. He proposed that the HClO_4 generated due to the interaction of AP and moisture may act as an excellent crosslinkage agent for double bonds. Myers⁽¹³⁾ also observed the hardening of the CTPB propellant, which he explained on the basis of cross-linkage reactions due to the oxidative attack of AP on CTPB double bonds. Layton^(14,16,17) proposed that the crosslinkages are formed along the polymer chains at the unsaturated sites, with the maximum percentage at the pendent vinyl groups.

Kishore, Verneker, and Prasad⁽¹⁸⁾ prepared and aged a PS/AP propellant in which they observed that the agency responsible for the ageing in the propellant is the thermal decomposition of the oxidizer contained in it. They determined that the rate-determining step in the propellant is the same as that in the AP decomposition in all of the temperature ranges studied.

Kishore, Verneker, and Prasad⁽¹⁹⁾ then prepared and aged two propellants under similar conditions. The propellants were AP/PS and NaCl/PS (control). After a period of ageing the AP/PS propellant had turned yellow homogenously throughout the bulk of the material, while

the NaCl/PS sample resembled that of the unaged propellant. The bulk portions of both propellants were analyzed by IR and the AP/PS sample showed the presence of a broad peroxy band while no such band was visible in the control. This experiment established that the oxygen for the oxidative attack on the binder comes from AP decomposition.

Kishore, Ravidran, and Sankaralingam(20) studied the slow decomposition of AP/PS propellant. The formation of benzaldehyde and benzoic acid was attributed to the formation of polystyrene peroxide (PSP) which then decomposed to the above products. The most plausible mechanism could be written as follows.



Layton(21) conducted an ageing study to evaluate and characterize the ageing behavior of HTPB propellants. It was shown that HTPB propellants obey the Layton ageing law as determined for the PBAN and CTPB composite propellants. The observed changes in mechanical properties were due to a chemical reaction occurring between the AP and the polymeric binder. A direct correlation between the change in

chemical crosslinks (from sol-gel measurements) and the mechanical properties supports the thesis that observed ageing changes are caused by chemical reaction. Because the rate of chemical reaction is controlled by a diffusion process, normal reaction kinetics do not apply. All the HTPB propellants were formulated with a chemical bonding agent that is designed to coat the AP oxidizer. Since the AP is responsible for the ageing reaction and the AP surface is coated in these HTPB propellants, it was assumed that the coating was responsible for a reduced ageing rate.

PART I. CARBON-13 NMR

Introduction

Polymer analysis by Carbon-13 NMR has had a primary emphasis in the study of polymeric composition, tacticity and dynamics in solution. However many polymers are insoluble and must be studied in the solid state and have greatest interest in terms of their mechanical properties. So far very few NMR studies of crosslinked polymer gels have been performed. This is due to the difficulty of preparing a physically homogeneous sample and that the line widths are much larger than in NMR spectra of the analogous linear soluble polymers at equal temperature and concentration.

When a linear polymer is cured, its molecular motion is severely restricted. Crosslinking restricts motion even more. This is reflected by the increased linewidths. Gray and Hill⁽²²⁾ state that curing a polymer does not grossly affect its overall chemical bonding characteristics.

In their paper⁽²²⁾ they state that the linewidths are a result of two major effects, the strong static magnetic interaction between the nucleus under observation and surrounding magnetic nuclei, and the spread of chemical shifts experienced by the observed nucleus because of the wide variety of orientations that it experiences with respect to the applied magnetic field.

Doskocilova and Schneider⁽²³⁾ performed ¹H-NMR on swollen crosslinked gels of various polymers. Their spectra of low crosslink

density samples exhibited a number of very narrow lines superimposed upon a very broad background. From these lines they determined the percentage of uncrosslinked "free" material present. They decided that the lines may correspond partly to signals of normal (linear) polymer, or "loose ends" of the polymer network, or partly to residual monomer. Possible information on the structure of the polymer based on "high-resolution spectra" may pertain only to a small fraction of the studied material.

Carbon-13 NMR has been widely used for investigating the microstructure of polybutadiene (PB). Mochel⁽²⁴⁾ observed that 1,2-PB displayed a set of chemical shifts completely different from that of 1,4-PB. He showed that in n-BuLi-catalyzed PB there are no cis-1,4-trans-1,4 linkages. Instead the polymer consisted of "blocks" of cis and trans units separated by isolated vinyl units.

Clague, Broekloven, and Blaauw⁽²⁵⁾ reported spectra of several sec-BuLi initiated PB's and their hydrogenated analogs, with various amounts of 1,2 structure, but with a roughly constant ratio of cis-1,4 and tras-1,4 structures. From the assignment of these spectra they showed that the cis- and trans-1,4 units are distributed in an essentially random manner and that 1,2 units are incorporated in a head to tail manner.

Furukawa, et.al.⁽²⁶⁾ did further work on an equibinary (50% cis and 50% trans) PB system. They refined the polymers chemical shifts and were able to assign the aliphatic region. The microstructure of this type of system was found to be composed of long cis blocks

separated by trans blocks. Thomassin, et.al.(27) also worked on this type of system and supported Mochel's assertions as to the block nature of this type of PB. IN a later paper, Mochel(28) presented 300 MHz ¹H NMR evidence for the presence of cis- trans-1,4 linkages and proved that his previous assumption was in error.

Gemmer and Golub(29) utilized NMR and IR to study the thermal oxidation of cis-1,4-PB. They found that although the oxidation of cis-1,4-PB was accompanied by extensive crosslinking with attendant insolubilization, it was found possible to follow the oxidation of the solid polymer directly with Carbon-13 NMR. The predominant products appearing in the spectra of oxidized polymer were epoxides. They found lesser amounts of alcohols, peroxides and carbonyl structures from complementary IR and NMR spectra of soluble extracts obtained from the oxidized, crosslinked cis-1,4 PB.

On the basis of previous work performed on PB, Ku(30) did a Carbon-13 NMR analysis of HTPB, CTPB, and hydrogenated HTPB polymers which had been polymerized via the free radical mechanism to give an average molecular weight of 3000. The relative abundance of the three types of structural units (cis-1,4, trans-1,4, and vinylic-1,2 units) were quantitatively determined and the distribution of the three units were found to be completely random. The amount of branching present was estimated to be less than 3%. Observed chemical shifts were found to be in general agreement with their calculated values.

Experimental

The solid propellant used in this study was from the Pershing I

missile and its composition is as follows: 10% HTPB; 65-70% AP (80% 200 μm + 20% 20 μm size particles), ~1% dioctyl adipate (plasticizer), ~1% isophorone diisocyanate [IPDI] and 16-18% Aluminum powder (10-20 μm). Pershing propellant samples from the same batch were also obtained after having been aged for 24 months at 75°F (23.9°C), 110°F (43.3°C), 130°F (54.4°C), 150°F (65.6°C), 170°F (76.7°C), and 190°F (87.8°C).

The Army prepared four reference mixtures (1,2,3,A) for the study and their compositions are given in Table I. Several homemade mixtures (I, VII, VIII), whose compositions are also given in Table I, were prepared and cured in test tubes at 83°C for 22 hours.

The propellants were stored and aged under several conditions in closed desiccators. The high temperature conditions were maintained in a drying oven and were used to prepare the aged samples. The conditions were as follows: 63°C at 50% humidity (HT &%), 63°C at 5% humidity (HT & L%), room temperature at 50% humidity (LT&H%), room temperature at 5% humidity (LT&%), and at room temperature and average humidity (RT).

The Carbon-13 NMR spectra were recorded on a JEOL FX-200 NMR Spectrometer at 50.10 MHz. Instrument conditions were as follows: pulse angle, 90°; pulse delay 2s; acquisition time, .34s; spectral width (unless noted), 12,000 Hz. Sample measurements were taken at 100°C with broad band decoupling.

To obtain the best spectral resolution a series of solvents and temperatures was tried upon the propellant samples. When the

Table I
Composition of Propellant Reference Mixtures

<u>Name</u>	<u>% HTPB</u>	<u>% AP</u>	<u>% Al</u>
Mix 1	17.4	82.6 75% 200 μm 25% 20 μm	--
Mix 2	22.2	77.8 (1 μm)	--
Mix 3	47.2%	--	52.8 (30 μm)
Mix A	12%	65-70% (bimodal)	16-18%

I	33.3%	66.7% (crystals)	--
VII	33.9%	66.1% (ground)	--
VIII	23.1%	41.0% (crystal)	35.9% (45 μm)

propellant was placed into DMSO-d₆ and run at 50°C there was no swelling of the sample and the observed resolution was poor. CDCl₃ offered improved resolution through increased sample swelling. A search of various solvents showed that s-tetrachloroethane offered the greatest amount of swelling with a high boiling point so that NMR spectral runs could be done at 100°C for increased chain mobility and improved resolution.

Propellant solutions for the Carbon-13 NMR measurements were prepared in s-tetrachloroethane, with concentrations of ≈40% by weight. The propellant was diced into ≈1 mm cubes for swelling in the tubes. Observed chemical shifts were referenced to an internal deuterated standard, d₂-s-tetrachloroethane. The number of transients taken for each spectrum varied from 5000 to 10,000. The degree of swelling of the polymer affected the observed intensity of the spectra with reproducible swelling difficult to obtain. Intensity measurements of the peaks were made from integrated areas and double checked by the cut-and-weigh technique.

Results and Discussion

Source of Carbon Spectrum. A proton spectrum of uncured HTPB is shown in Figure 1. The spectrum has poor spectral resolution for the various structural components present in the polymer chain. The carbon-13 spectrum of HTPB is shown in Figure 2. As can be seen, the spectrum consists of two main regions, the unsaturated or vinylic region from 114 to 155 ppm and the saturated carbon region from 24 to

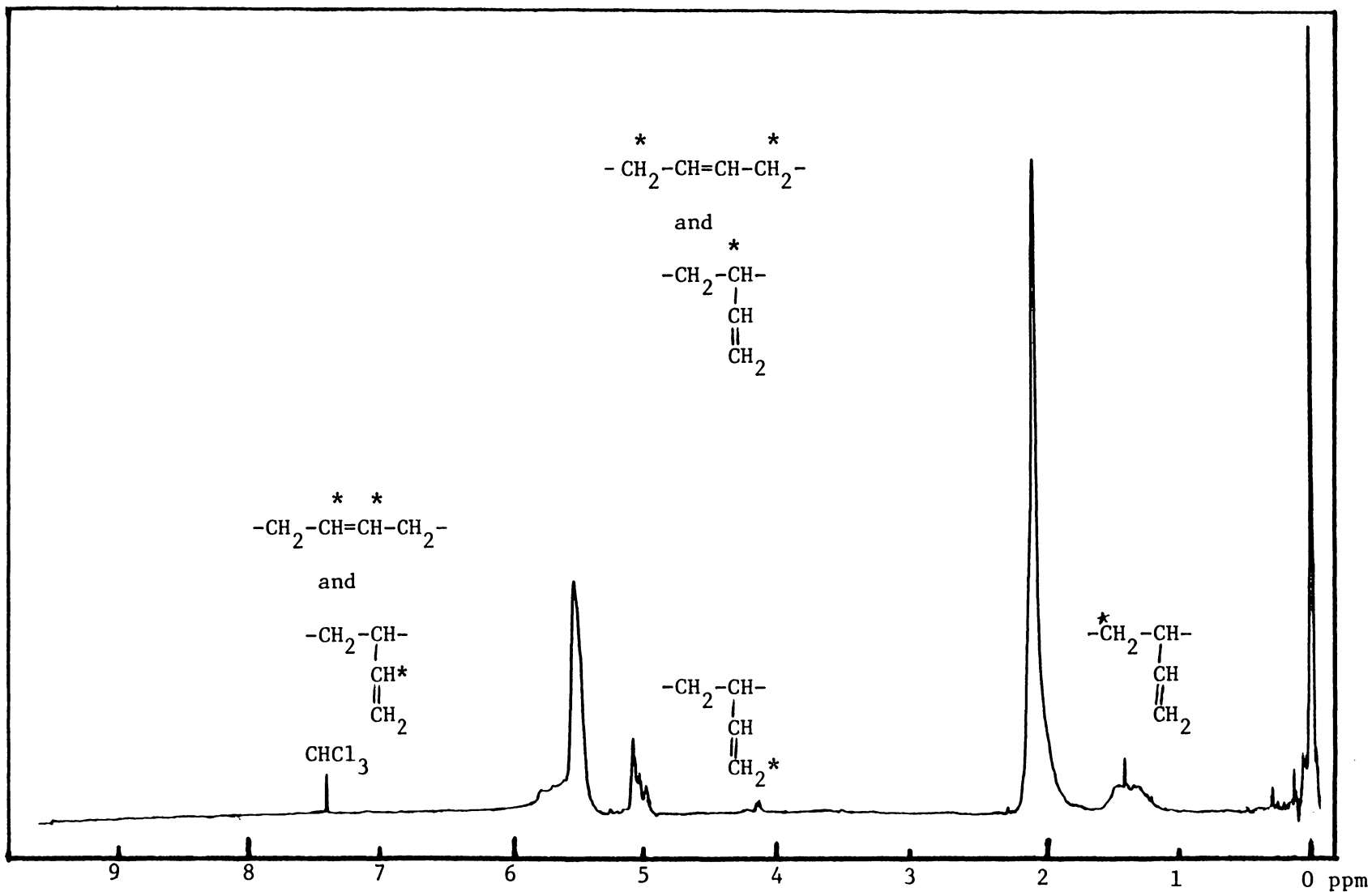


Figure 1. Proton NMR Spectrum of HTPB

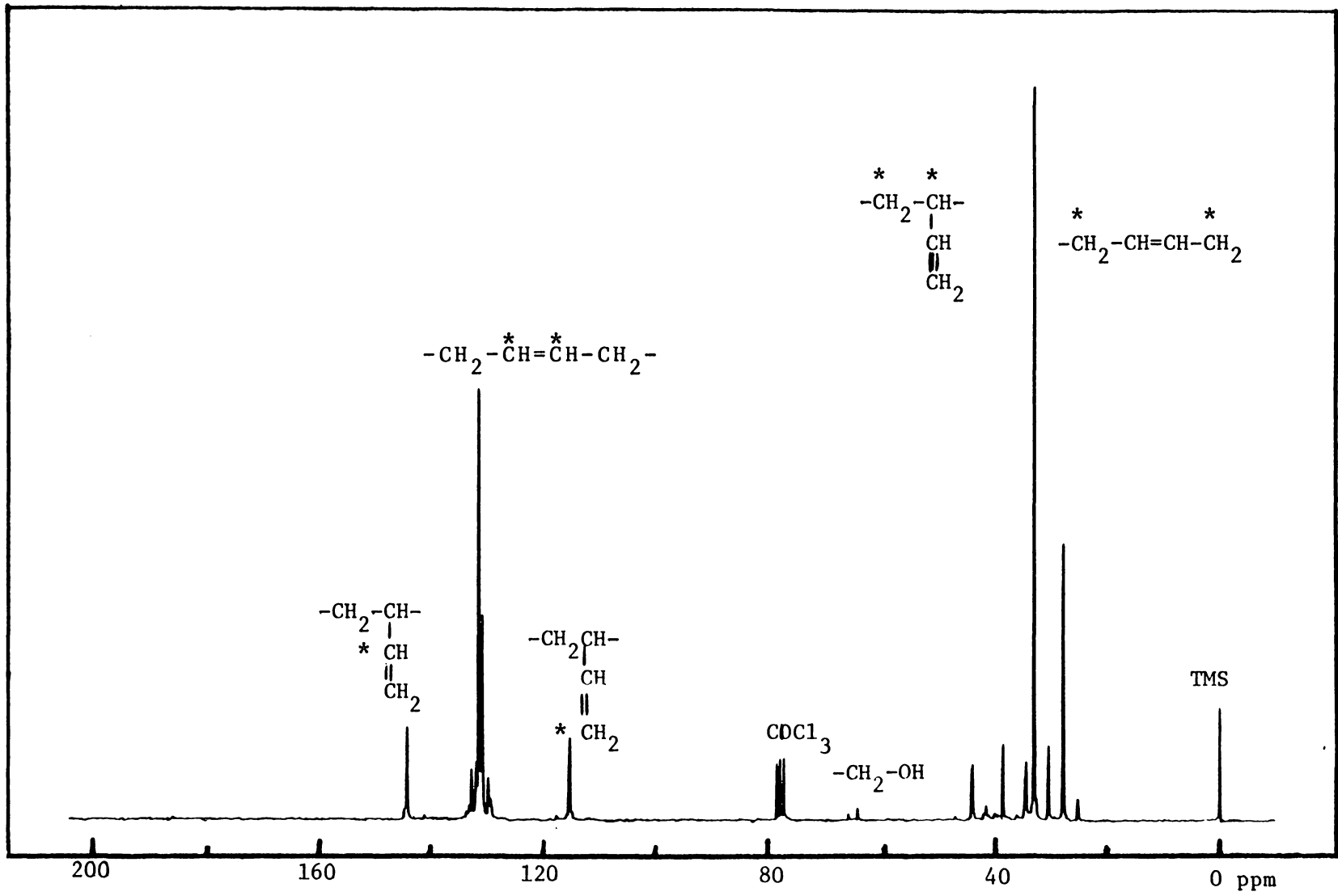


Figure 2. Carbon-13 NMR Spectrum of HTPB

44 ppm. The hydroxyl-bearing terminal carbons appear as weak resonances in the 63 to 65 ppm region. Figures 3 and 4 are expansions of the saturated and unsaturated regions respectively. The chemical shifts were found to be in agreement with those observed and calculated by Ku(30).

With curing and the combination of HTPB into a propellant there is a significant loss of spectral resolution. Due to this, the carbon-13 work was concentrated on the series of samples which had been aged at high temperatures for two years as they would most likely show the greatest amount of change.

In running a carbon-13 spectrum of a polymer one needs to determine whether the source of the signal is from the polymer chain itself or from the unpolymerized monomers trapped in the polymer matrix. For any carbon-13 analysis of a polymer this is a serious question but for the analysis of this type of propellant it is not relevant. The properties of the propellant depend upon its total composition. It is therefore necessary for the carbon-13 analysis to include all resonance sources which are present in a sample.

The spectral appearance of the 190°F aged sample in Figure 5 is characteristic of all the Pershing propellant samples. The peak at 130 ppm is due to the cis and trans vinyl units on the polymer backbone and the resonances at 114 and 142 ppm are due to the pendant vinyl groups. The saturated carbon region is less defined with two discernable peaks present on a broad hump. The peak at 74.0 ppm is due to the solvent resonance of s-tetrachloroethane. When comparing Figures 2 and 5, the

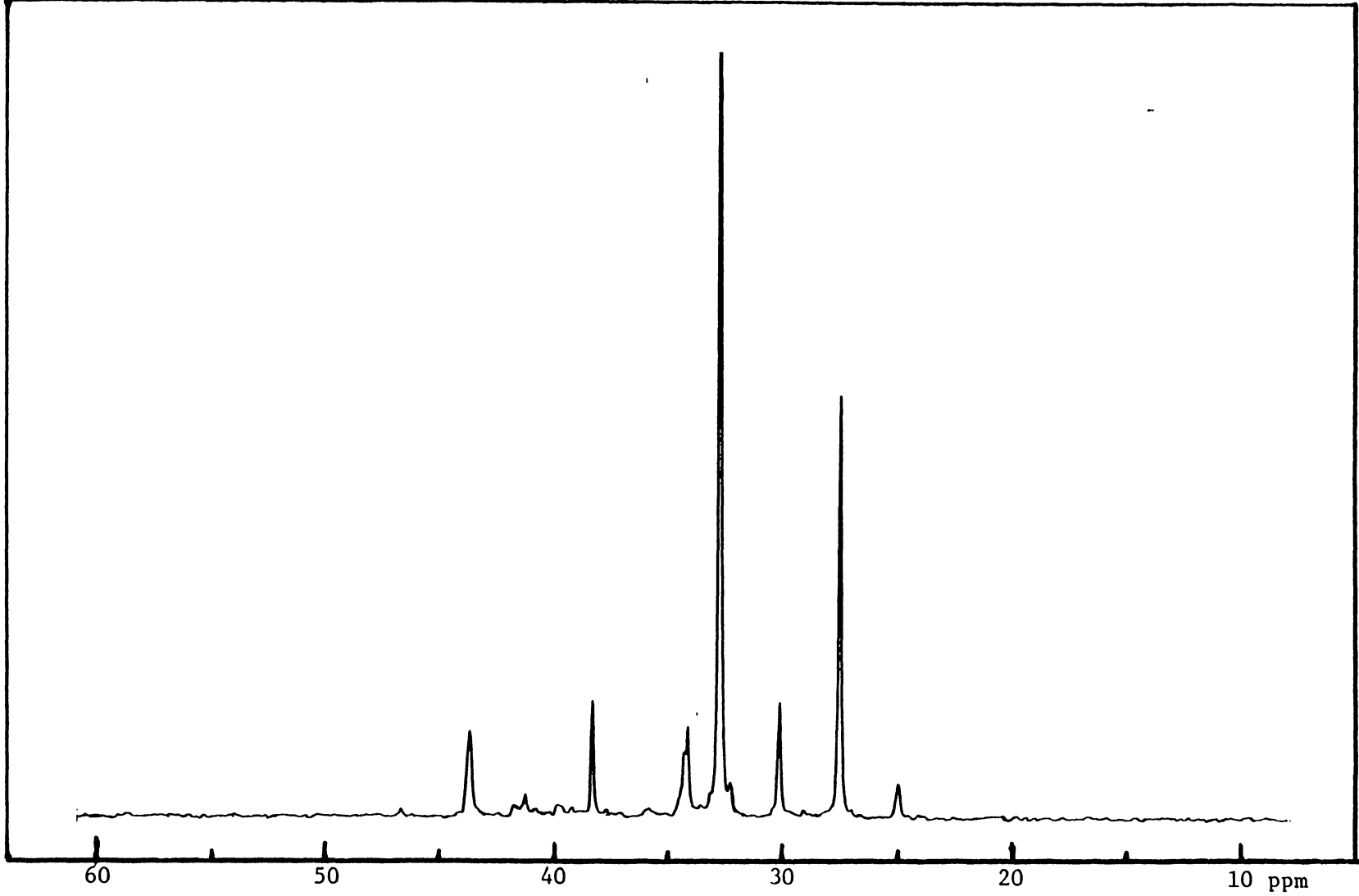


Figure 3. Saturated Carbon Region of HTPB

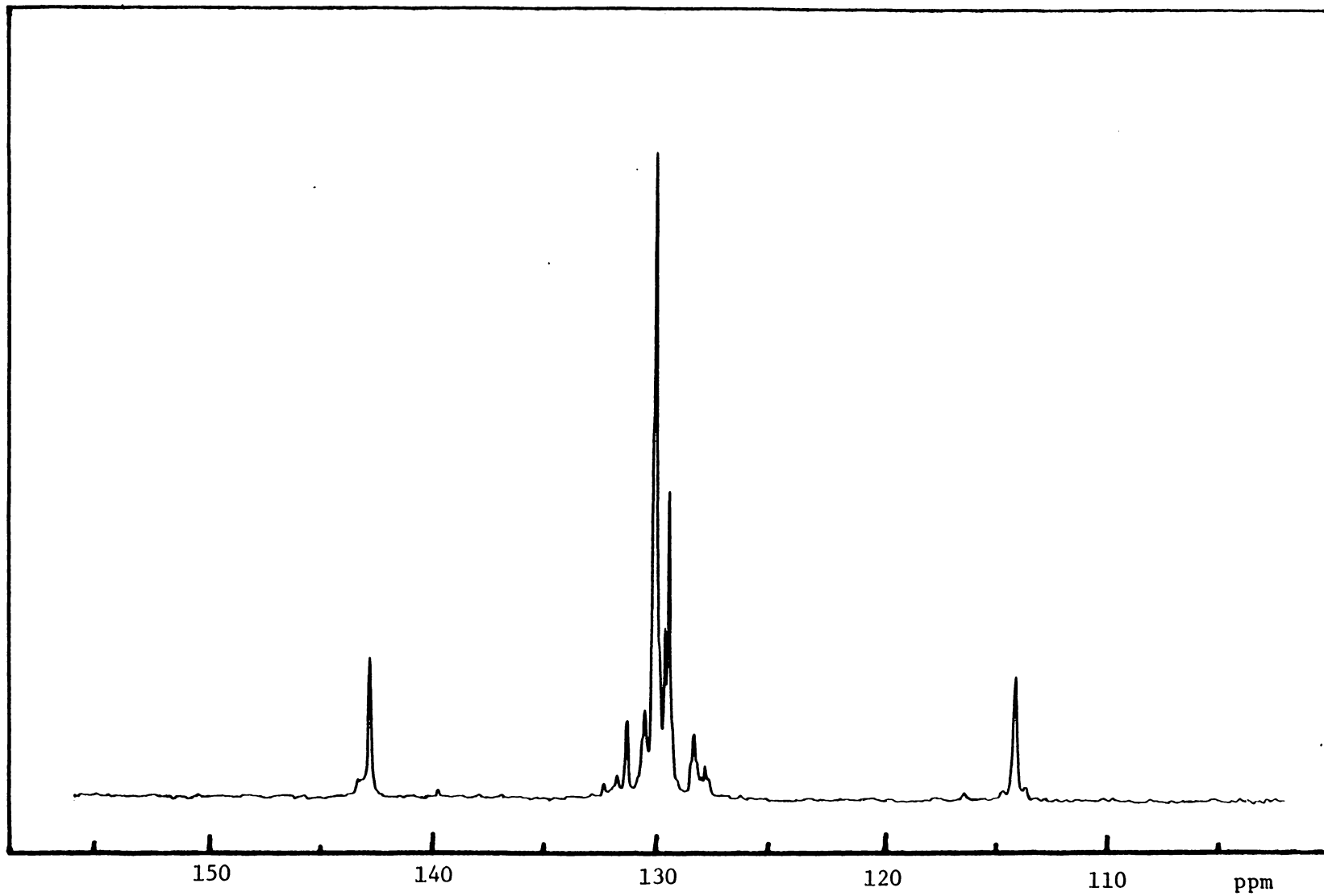


Figure 4. Unsaturated Carbon Region of HTPB

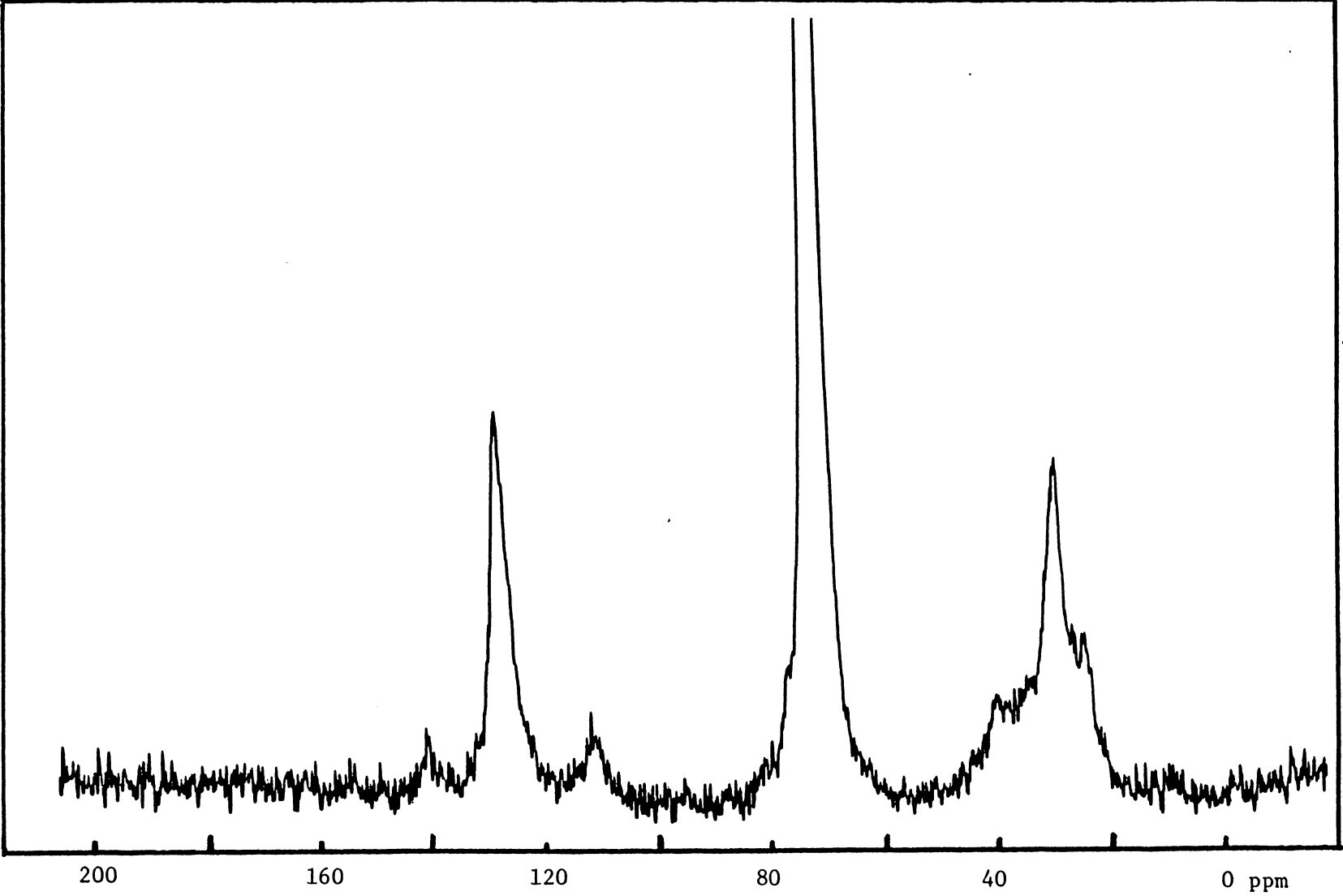


Figure 5. Carbon-13 Spectrum of Propellant Aged at 190°F for 24 Months

loss of resolution due to curing and propellant formulation is quite evident. To investigate the contribution of the extractable portion of the propellant system to the carbon-13 signal, the liquid from Figure 5's sample was run and this spectrum is shown in Figure 6. This spectrum shows that the extractable portion does contribute to the observed signal. The amount of contribution is in doubt since the reswelled propellant spectrum, shown in Figure 7, has such low intensity. This is due both to the loss of most of the extractables and the increased swelling for the sample during the run. A question which has not been answered by this investigation is whether there are more extractables being formed by the ageing process.

In Table II the peak positions for the aged propellant samples are given. As can be seen almost all values are within experimental error of each other in both the vinylic and saturated regions. The exception is in the vinylic region for the 2 year aged sample at 190°F. The shift of the resonance from 129.71 ppm to the 130.1 and 131.4 ppm area probably indicates that there are more trans-vinylic linkages present in the polymer backbone. There appears to have been a preferential loss of some of the cis-linkages over the trans-linkages.

Vinylic Content Analysis. The ratio of the saturated to vinylic carbons was studied for any systematic changes. As seen in Figure 8, 9, and 10 the carbon-13 spectrum for propellants aged at different temperatures appear quite similar. By using the integrated peak areas,

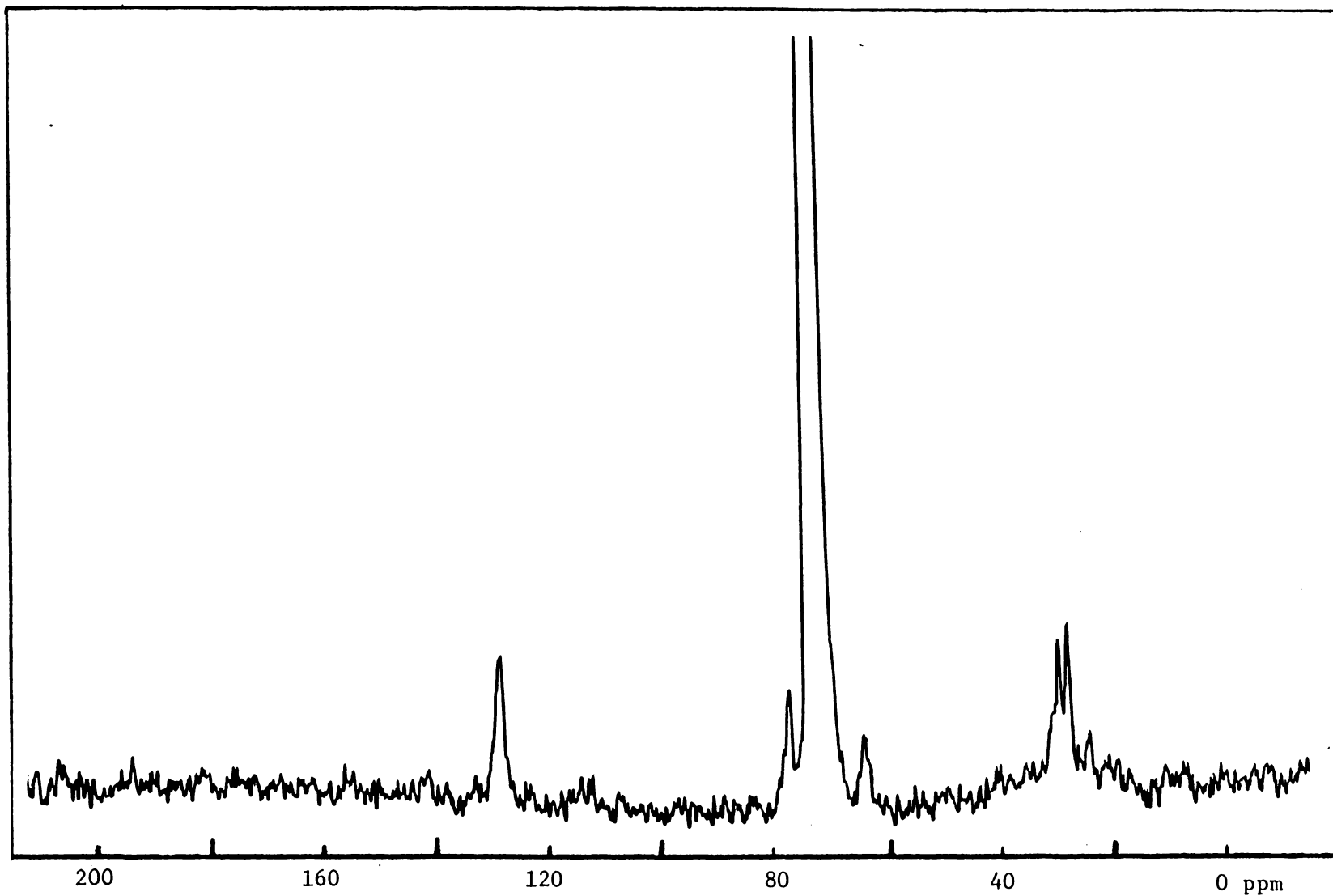


Figure 6. Carbon-13 Spectrum of Extractables from the 190°F Propellant

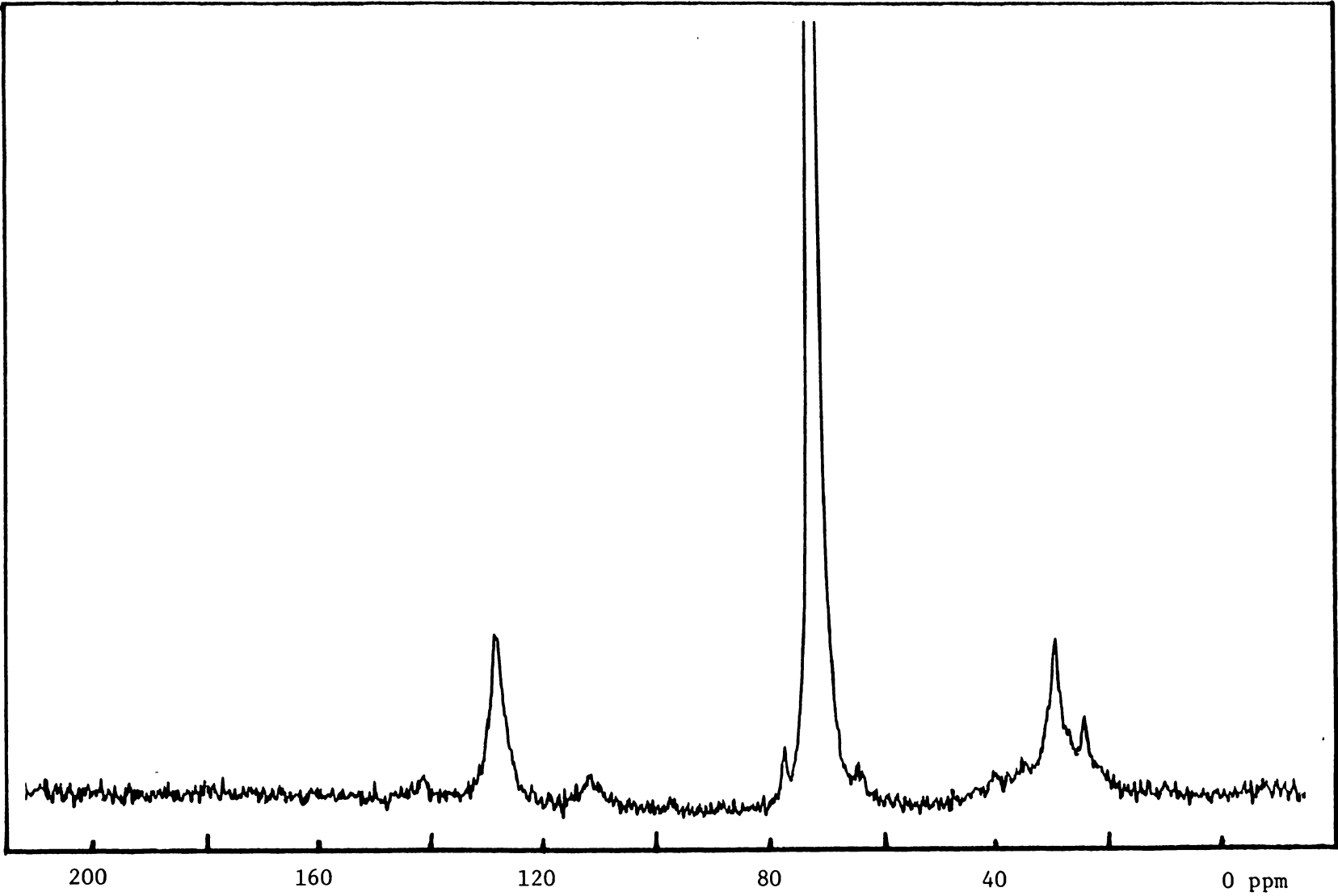


Figure 7. Carbon-13 Spectrum of Reswelled Propellant (190°F)

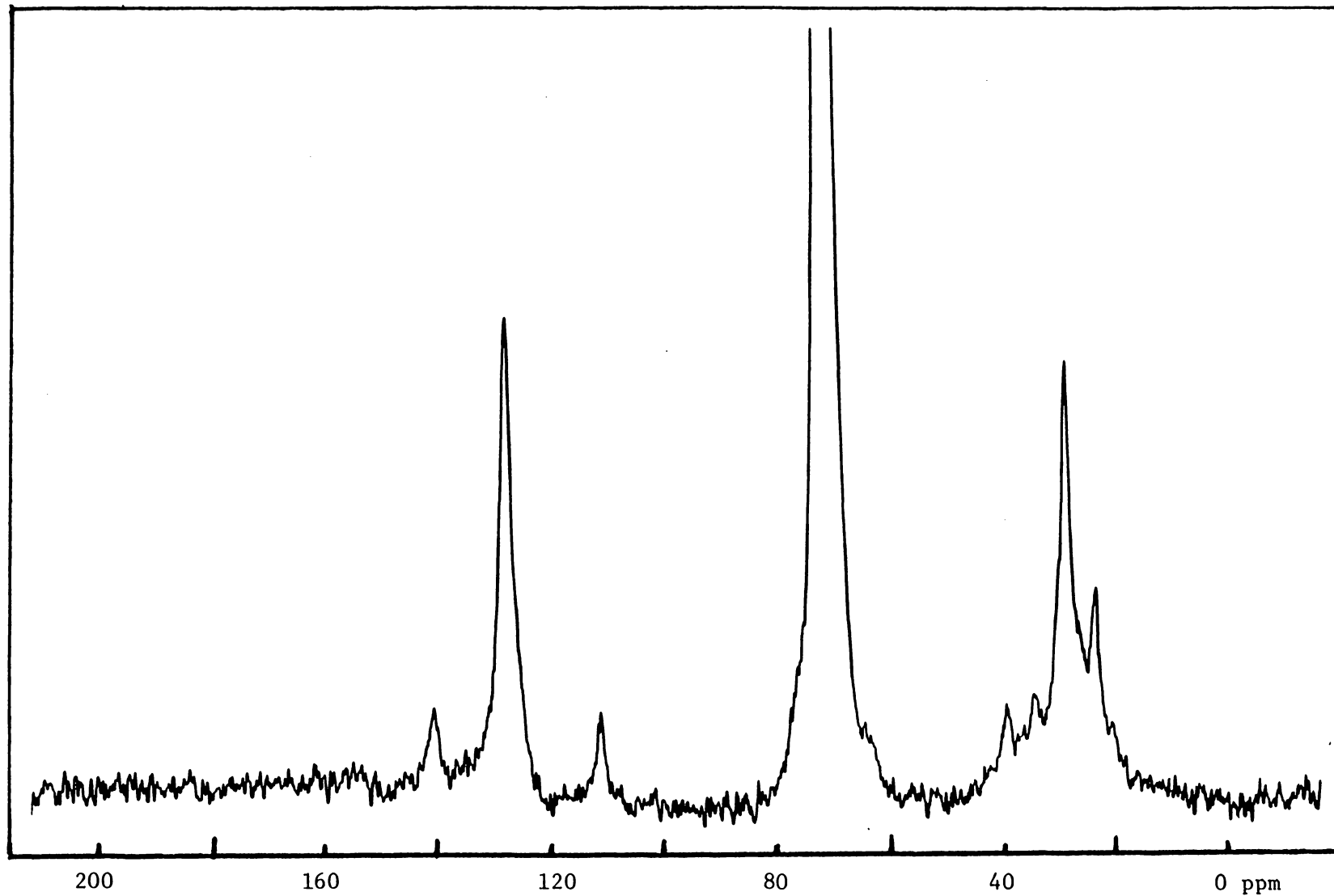


Figure 8. Carbon-13 Spectrum of Propellant Aged at 75°F for 24 Months

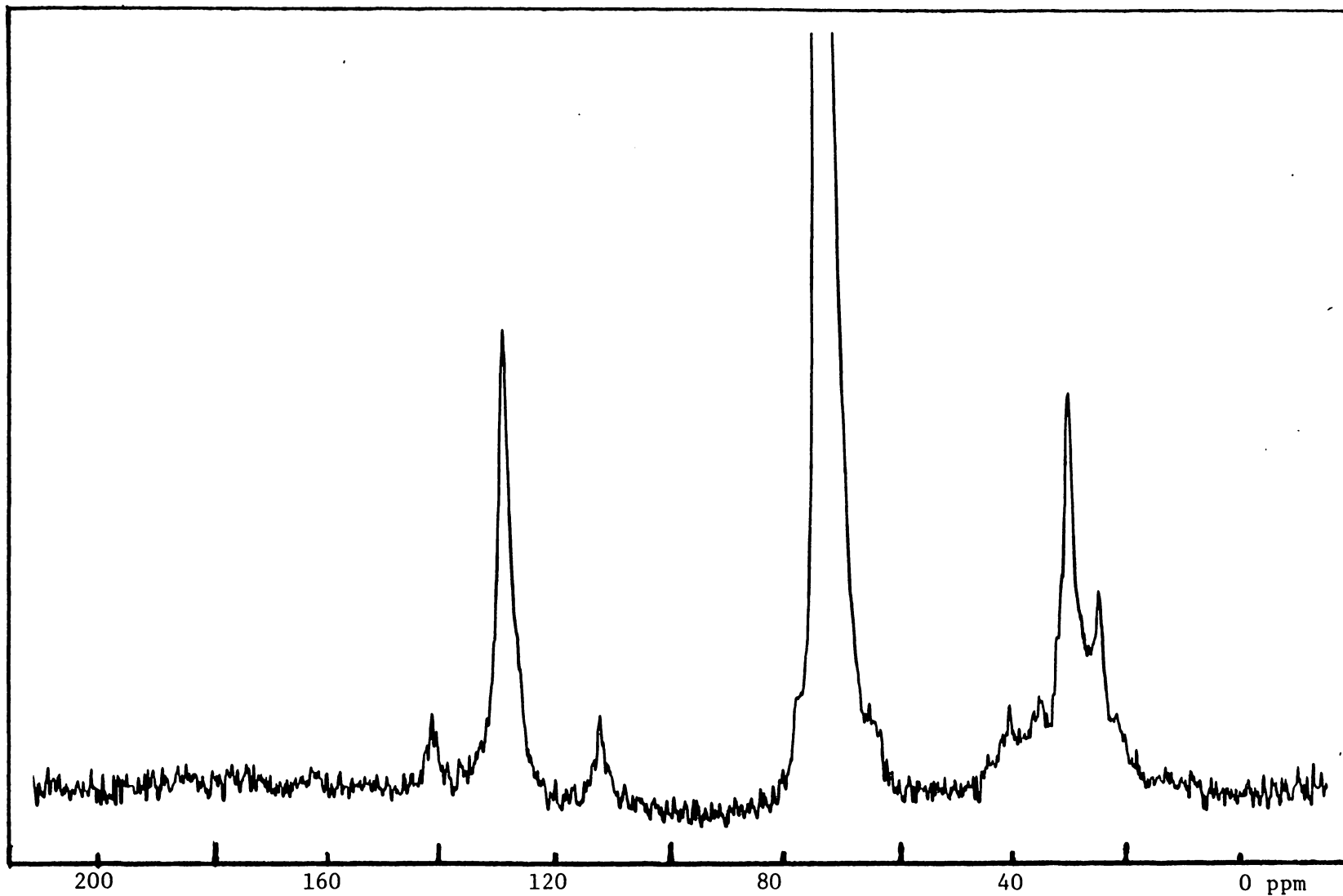


Figure 9. Carbon-13 Spectrum of Propellant Aged at 110°F for 24 Months

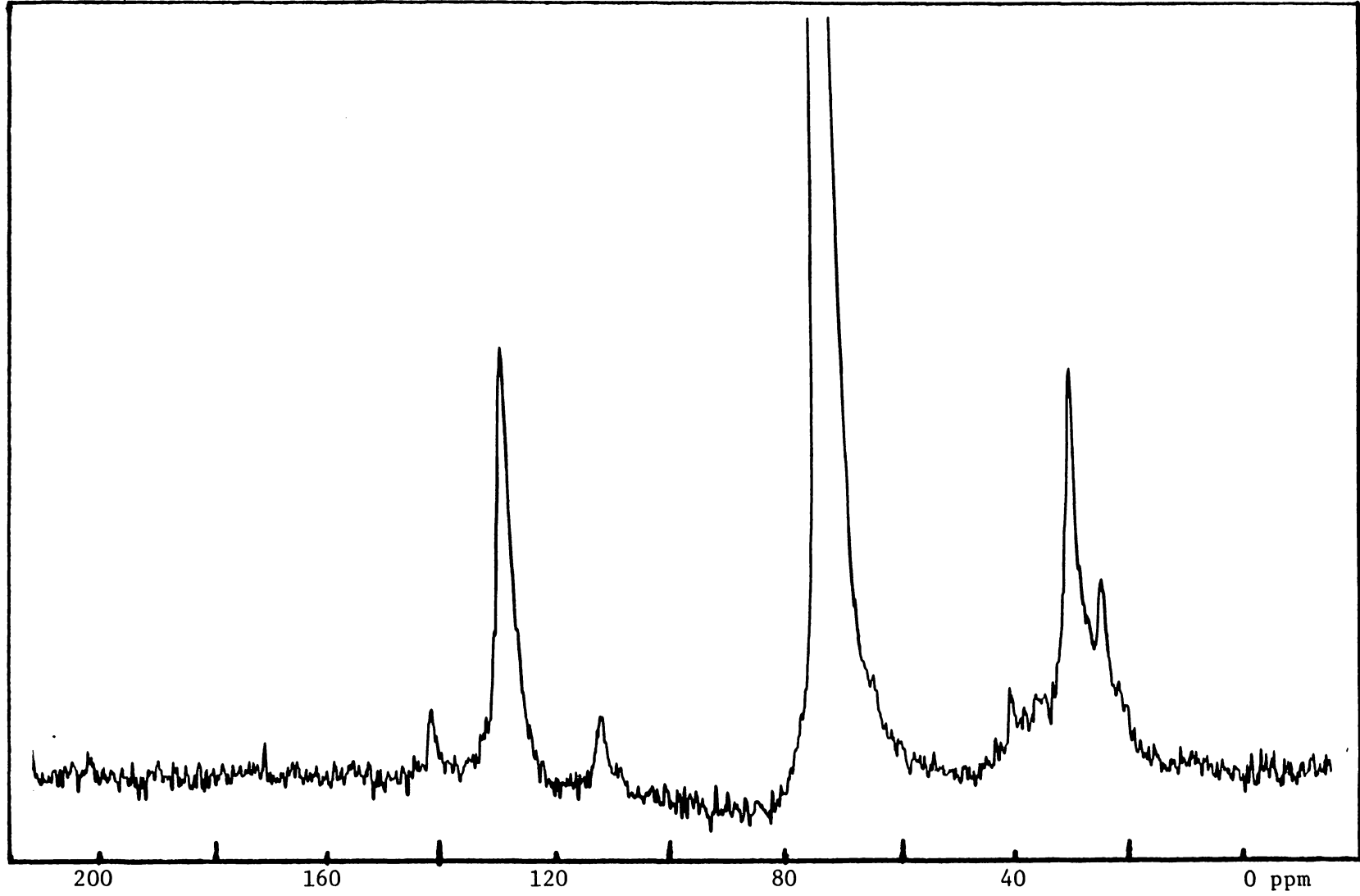


Figure 10. Carbon-13 Spectrum of Propellant Aged at 150°F for 24 Months

Table II
Comparison of Carbon-13 Peak Positions

<u>Sample</u>	<u>Major Peak Positions (PPM)</u>					
75°F	27.0	32.2	74.0	114.1	129.7	142.7
110°F	27.3	32.3	74.0	113.8	129.7	142.6
150°F	27.2	32.2	74.0	113.9	129.7	-----
190°F	27.3	32.3	74.0	113.6	130.1 131.4	142.6

differences between the spectra could be noticed. The peak area percentages of the vinylic components and the vinylic/saturated ratio are shown in Table III. As can be seen the extractables from the 190°F aged sample have the same proportional vinylic content as the whole propellant but the vinylic/saturated ratio is considerably lower. This can be attributed to the measurement error incurred due to the low signal-to-noise ratio.

In Table III there are two noticeable trends. The first is that there is an increasing loss of the vinyl groups as the sample is aged at higher temperature. The other trend complements the first in that the percentage of pendant vinyl carbons at 142 and 114 ppm decreases with increasing ageing temperature. This shows that there is a preferential loss of pendant vinyl groups over those in the polymer backbone. From the data in both Tables II and III, the preference for vinylic group loss could be given as pendant >> cis > trans.

Of concern is that the integrated vinyl/saturated carbon ratio is not near its theoretical value of 1.0 for the unaged samples. Integration of Ku's⁽³⁰⁾ pure cured HTPB spectra show the ratio to be around 0.96, close to the theoretical value of 1.0. It could appear that the vinylic loss occurs at a given rate once the propellant is formed and that the rate is increased for samples stored at higher temperatures. Another consideration for the lowered ratio is that the vinylic carbons did not have sufficient time to relax completely between the RF pulses. This would cause a lowering of the observed intensity for a peak but due to the experimental conditions this should

Table III
Vinyllic Character of the Propellant

<u>Sample</u>	<u>% of Total Unsaturated Content</u>			<u>Total Vinyllic Total Saturated</u>
	<u>142PPM</u>	<u>130PPM</u>	<u>114PPM</u>	
75 F	9.7	82.1	8.2	0.753
110 F	8.5	83.6	7.9	0.742
150 F	7.6	84.7	7.7	0.736
190 F (Rinsed)	6.1	87.5	6.4	0.720
190 F	7.4	82.0	10.6	0.763
190 F (Extract)	6.8	82.3	10.9	0.469

not be a factor.

For the Pershing propellant samples aged under low and high temperature conditions in the laboratory the same two vinylic trends are present. There is a loss of vinylic groups with a preference for the loss of pendant vinyl groups. It should also be noted that no resonances corresponding to epoxides, peroxides, or alcohols were observed. If these oxidation products are present then they are not present in detectable quantities with current procedures and instrumentation.

Summary

In summary, carbon-13 NMR of the aged Pershing propellant samples has shown that with increasing ageing temperature there is a corresponding increase in the loss of vinylic groups. It has also shown that this loss of vinylic groups is preferential in the order pendant >> cis > trans.

PART II. PHOTOELECTRON SPECTROSCOPY

Introduction

XPS is used in the determination of the molecular structure of organic and inorganic compounds. Observable shifts in the electron binding energy will occur owing to differences in the chemical environment about the atom of interest. Lindsay and coworkers⁽³¹⁾ studied the structural effects on the "chemical shift" of various aluminum oxides. They found that the Al(2p) peak in α -Al₂O₃ (corundum) occurs at 76.3 e.v., relative to a gold reference peak. Nefedov and his coworkers⁽³²⁾ reported a shift of 2.7 e.v. for α -Al₂O₃ relative to aluminum metal, with the C(1s) line as standard. Barrie⁽³³⁾ also reported a shift of 2.7 e.v. for Al₂O₃ (75.3 e.v.) on an evaporated Al (72.6 e.v.) surface.

A literature survey reveals no specific work on AP, but work has been done on other perchlorates. Prins⁽³⁴⁾ investigated the photoelectron spectra of a series of oxyanions for information on the type of bonding present. A result of this study was that it was found that ClO₂⁻ decomposed under the x-ray flux to ClO₃⁻ and Cl⁻. They found that LiClO₂ decomposed faster than NaClO₂ and that there was minor decomposition of ClO₃⁻ to Cl⁻ after 15h irradiation.

In a number of papers, Copperthwaite and Lloyd^(35,36,37) studied the photoinduced decomposition of NaClO₄ and NaClO₃ by XPS. It was shown that the process, which probably occurs as follows ClO₄⁻ → ClO₃⁻ → Cl⁻, is a consecutive first order one for exposure times of less than

$1.5t^{1/2}$. The process is accompanied by evolution of clathrated molecular oxygen which suggested that the final irradiation product, NaCl, has gross defects in structure in the surface regions.

The lineshapes obtained in the XPS analysis of polymers tend to be symmetric and have constant linewidths. This allows the component signals to be approximated by Gaussian lineshapes and quite detailed curvefitting becomes possible. Clark and coworkers(38,39,40) have produced a series of XPS studied on polymers and multipolymer systems. Through curve deconvolution techniques they have compiled tables of binding energies of C(1s), O(1s), N(1s), and Cl(2p) levels for typical structural features of common occurrence in polymer systems.

Experimental

Spectra were obtained using a DuPont 650 Electron Spectrometer with a Mg anode. Slices of the propellant were mounted on a brass probe with double-sided scotch tape. Due to the decomposition of the perchlorate, sample outgassing was considerable. The X-ray source was operated at 10 KV and 19 mA under a typical pressure of 9×10^{-7} torr. The peak positions were referenced to the contaminating C(1s) peak at 284.0 ev. In the usual operating procedures narrow scan spectra of a sample were obtained in the following order: C(1s), Cl(2p), N(1s), O(1s), C(1s). The amount of time the sample was under x-ray flux before the Cl(2p) spectrum was collected was also recorded. Occasional long period scans were done to observe the Al(2p) region. In several runs, the Cl(2p) and the N(1s) peak was monitored as a function of

x-ray flux exposure time. Ratios of the amounts of an element present were obtained by measuring the respective peak heights.

Due to instrumental problems the last set of spectra were obtained using a Physical Electronics 550 ESCA/SAM operating with a Mg anode at 10 KV and 40 MA at a pressure of 10^{-8} torr. The data was processed using a DEC PDP 11/04 computer. The spectra were smoothed and referenced to the C(1s) peak at 284.0 ev.

Scanning Electron Microscopy (SEM) of the propellant surface was done using an Advanced Metals Research Corporation Model 900 scanning electron microscope operating at 20 kV. Photomicrographs of two propellant samples were taken at 170X and 850X magnification. Energy dispersive x-ray analysis (EDAX) of the embedded particles was performed using an International Model 707A unit attached to the microscope.

Results and Discussion

In the XPS portion of the study, reference compounds and their spectra were obtained for identification purposes. Figure 11 shows the spectrum of pure AP powder for the Cl(2p) photopeak. For the Cl⁺⁷ state the peak is located at about 208.5 ev. Note that the Cl photopeak is composed of a pair of overlapping peaks due to the two spin states of the P orbital. The small hump at 200.0 ev is composed of two x-ray satellite peaks due to the $K_{\alpha 3}$ and $K_{\alpha 4}$ x-rays from the Mg source. The two satellite peaks are 8.0 and 4.1% as intense as the parent peak. The N(1s) photopeak of AP appears at 402.0 eV as shown in Figure 12, while Figure 13 shows the Cl(2p) spectrum for NH₄Cl. Here

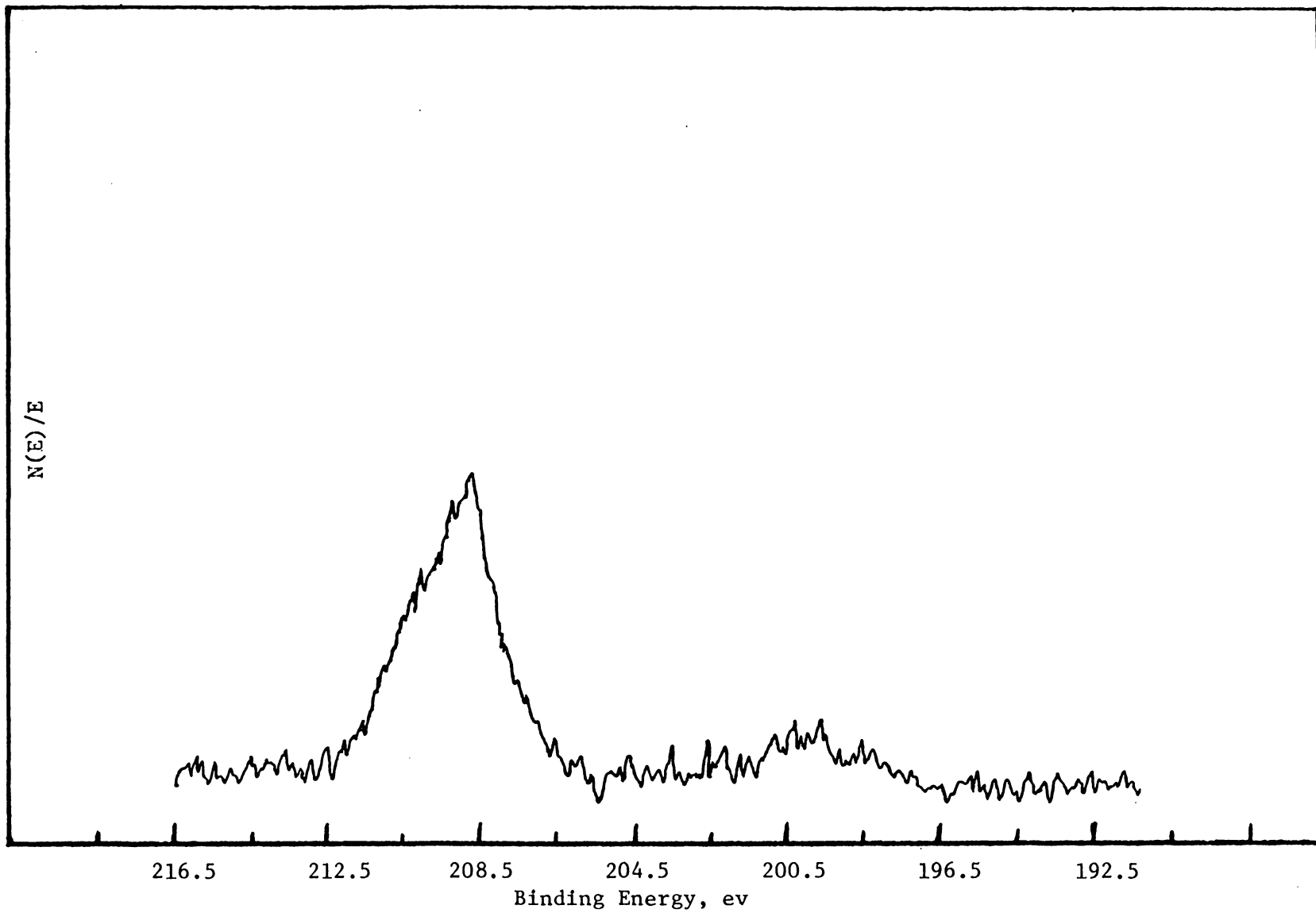


Figure 11. XPS Cl(2P) Spectrum of AP

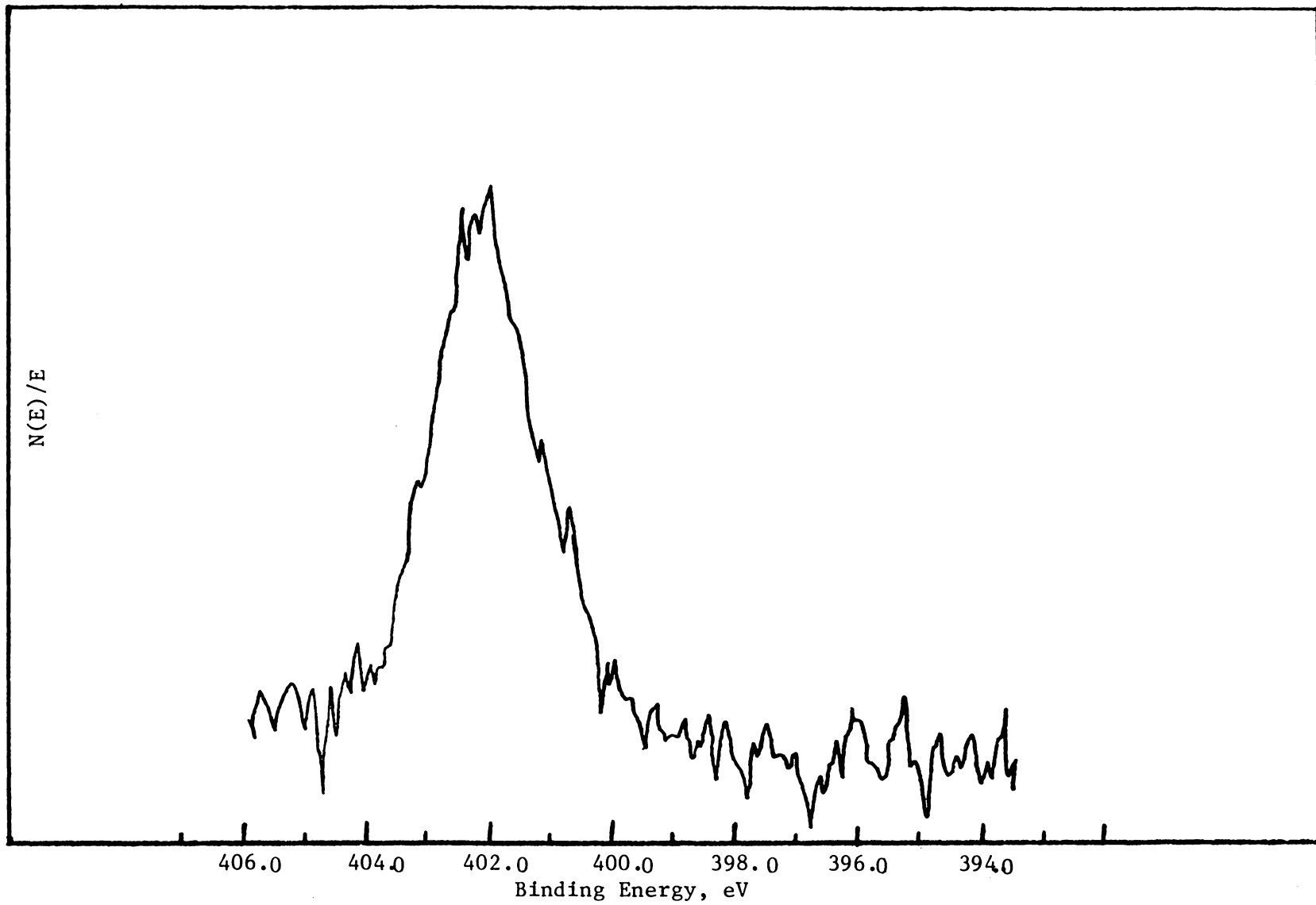


Figure 12. XPS N(1s) Spectrum of AP

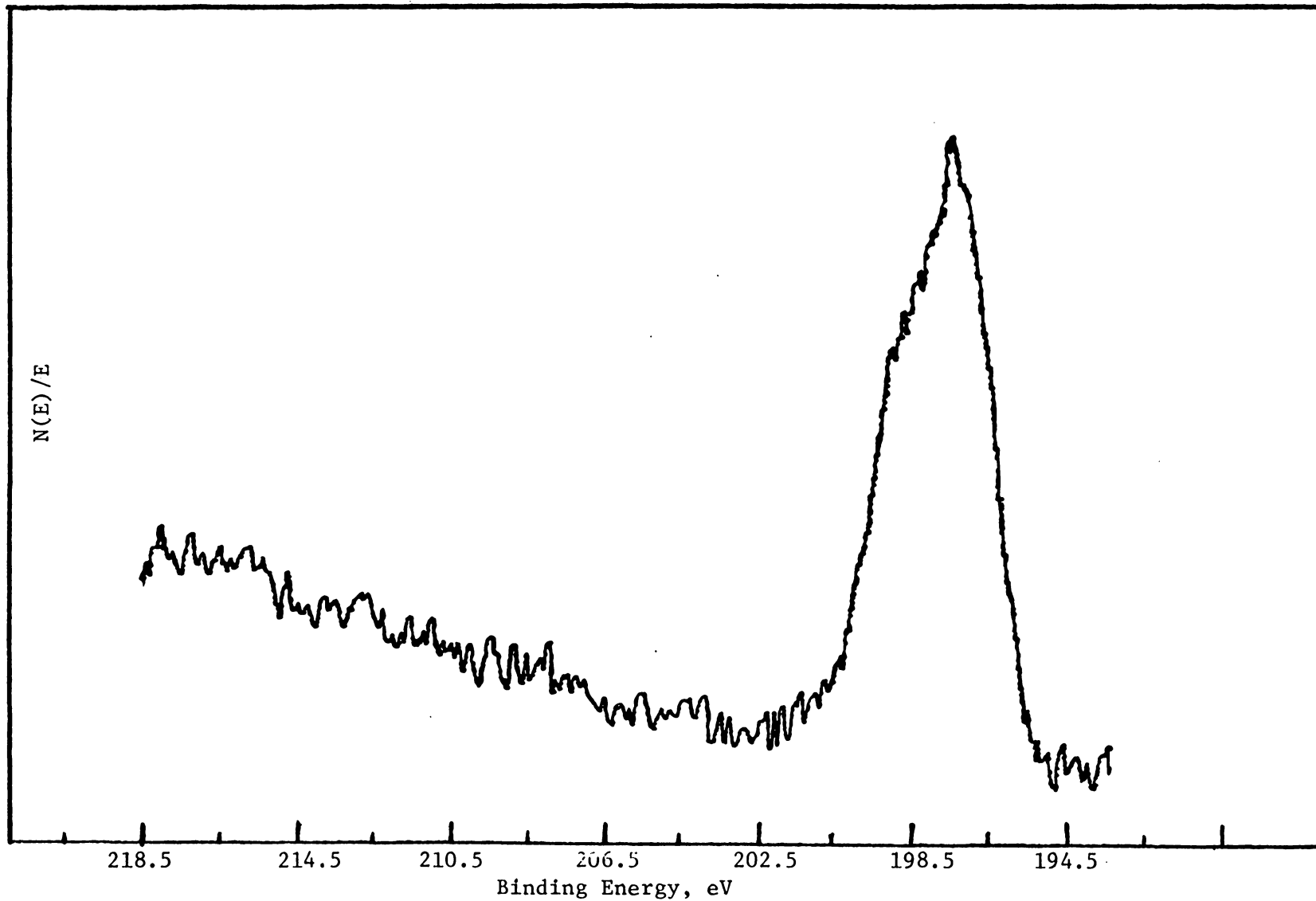


Figure 13. XPS Cl(2p) Spectrum of NH₄Cl

the Cl^- state is located at about 197.1 eV. The $\text{N}(1s)$ photopeak at 399.4 eV from cured HTPB is shown in Figure 14. The separation of the $\text{N}(1s)$ peaks due to AP and cured HTPB allows one to investigate relative changes in peak intensity from these two sources. A typical 1000 eV wide scan of the propellant is shown in Figure 15, with typical $\text{O}(1s)$ and $\text{C}(1s)$ spectra in Figure 16 and 17 respectively.

X-Ray Degradation of AP. As Copperthwaite and Lloyd(35,36,37) have shown, AP decomposes to NH_4Cl under the x-ray flux conditions of XPS. This was checked on the instrument used for this study. Figure 18 shows this degradation over a period of 73 minutes for ground AP crystals. This photoreduction degradation also occurs in various HTPB-AP mixtures as Figures 19 through 22 show. A comparison of the degradation rates between different samples probably is not possible due to changing instrumental parameters (primarily due to different x-ray fluxes depending upon the anode's condition) but as Figure 23 shows that the formation of NH_4Cl due to x-ray degradation is slower for AP in unaged (LT & %) and aged (HT & %) propellant samples than for pure AP. This can be attributed to the PB coating the AP particle and decreasing the x-ray flux to the particles. The $1\ \mu\text{m}$ AP particles have been coated with an aziridine complex to slow the degradative processes in a propellant system. This is reflected by the reduced amount of NH_4Cl formed under XPS conditions for a given time period.

SEM of Propellant Surface. Since XPS is a surface technique, it is necessary to have an idea of the surface appearance. The SEM photomicrographs, Figure 24 and 25, show the surface of a slice of

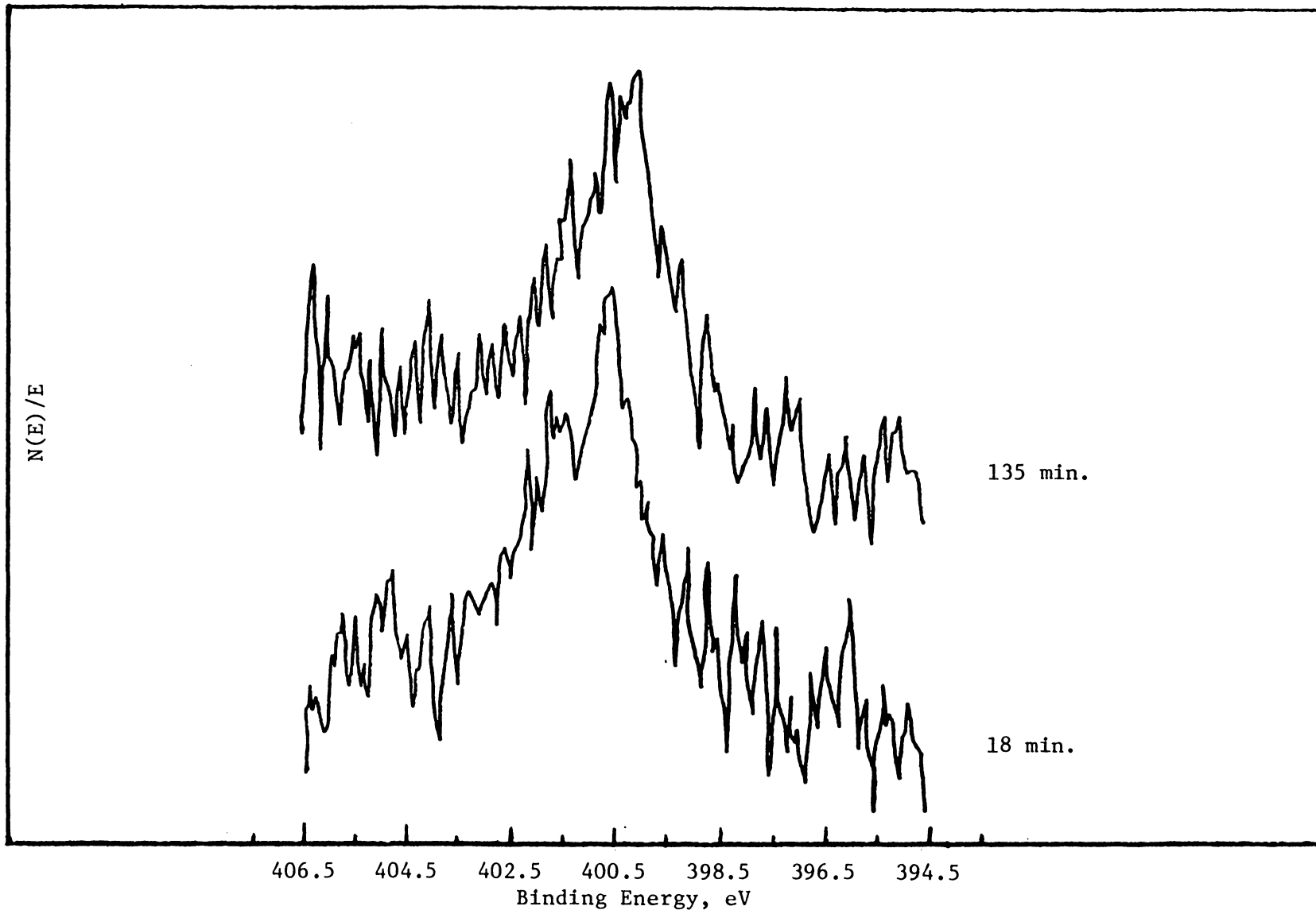


Figure 14. XPS N(1s) Spectrum of HTPB

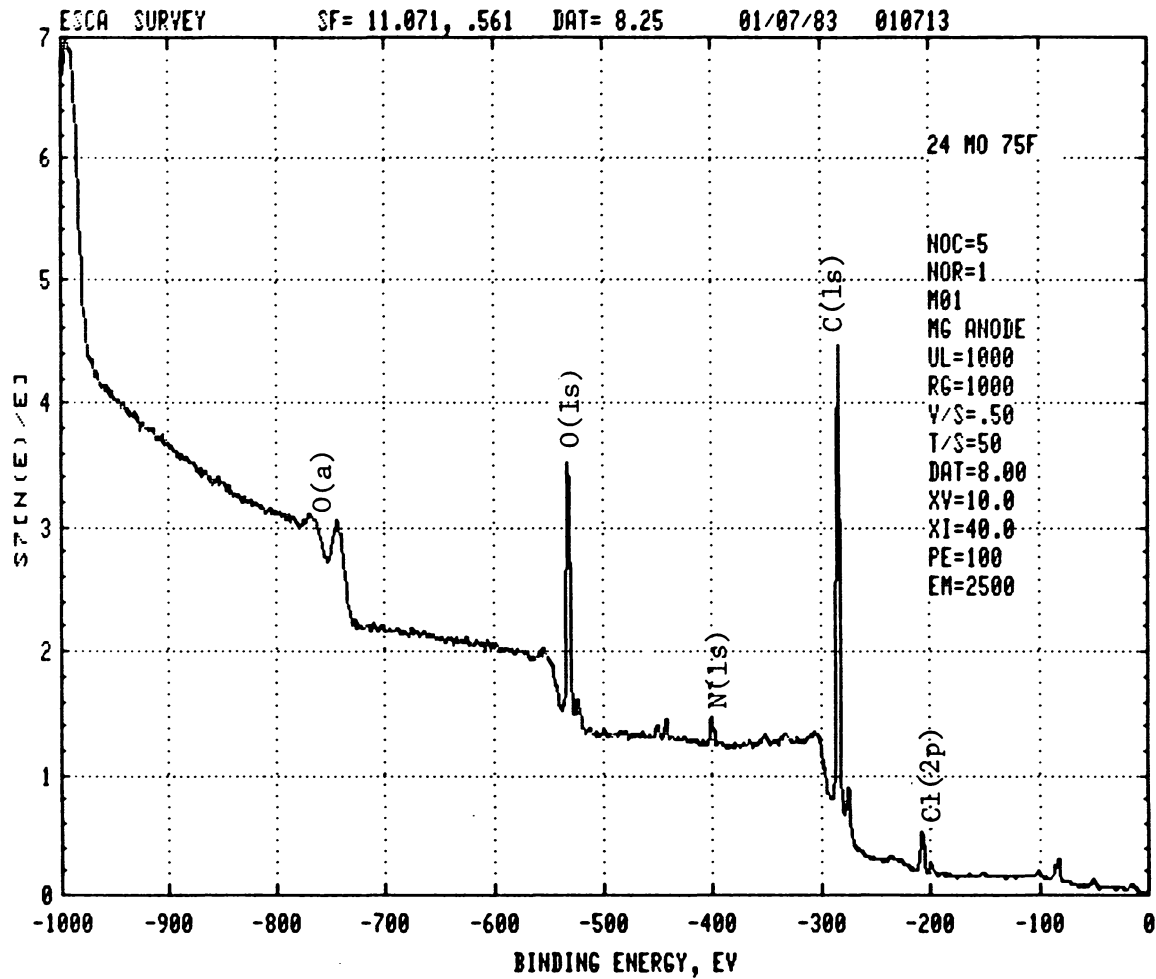


Figure 15. XPS Widescan Spectrum of Propellant Aged at 75°F for 24 Months

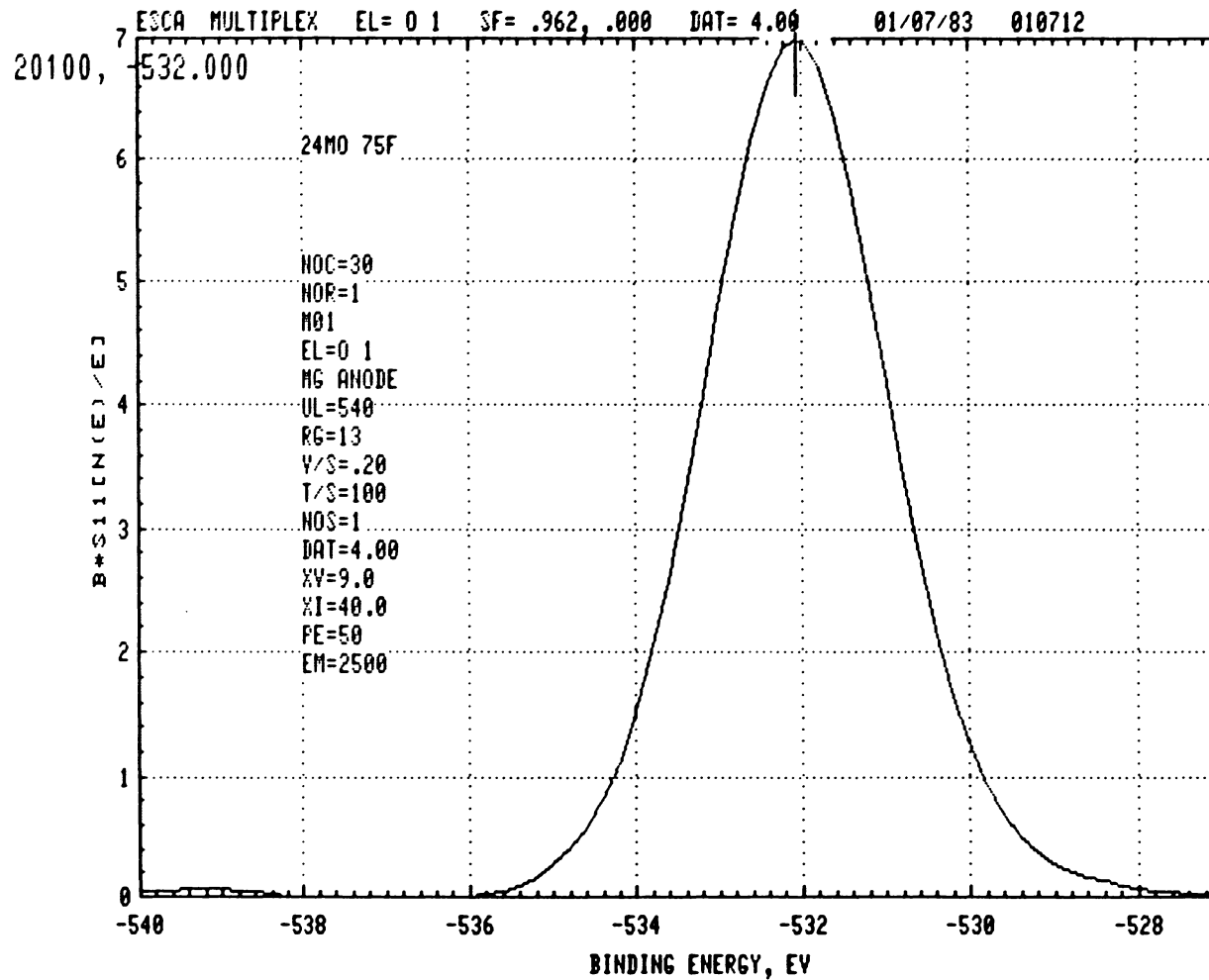


Figure 16. XPS O(1s) Spectrum of Propellant Aged at 75°F for 24 Months

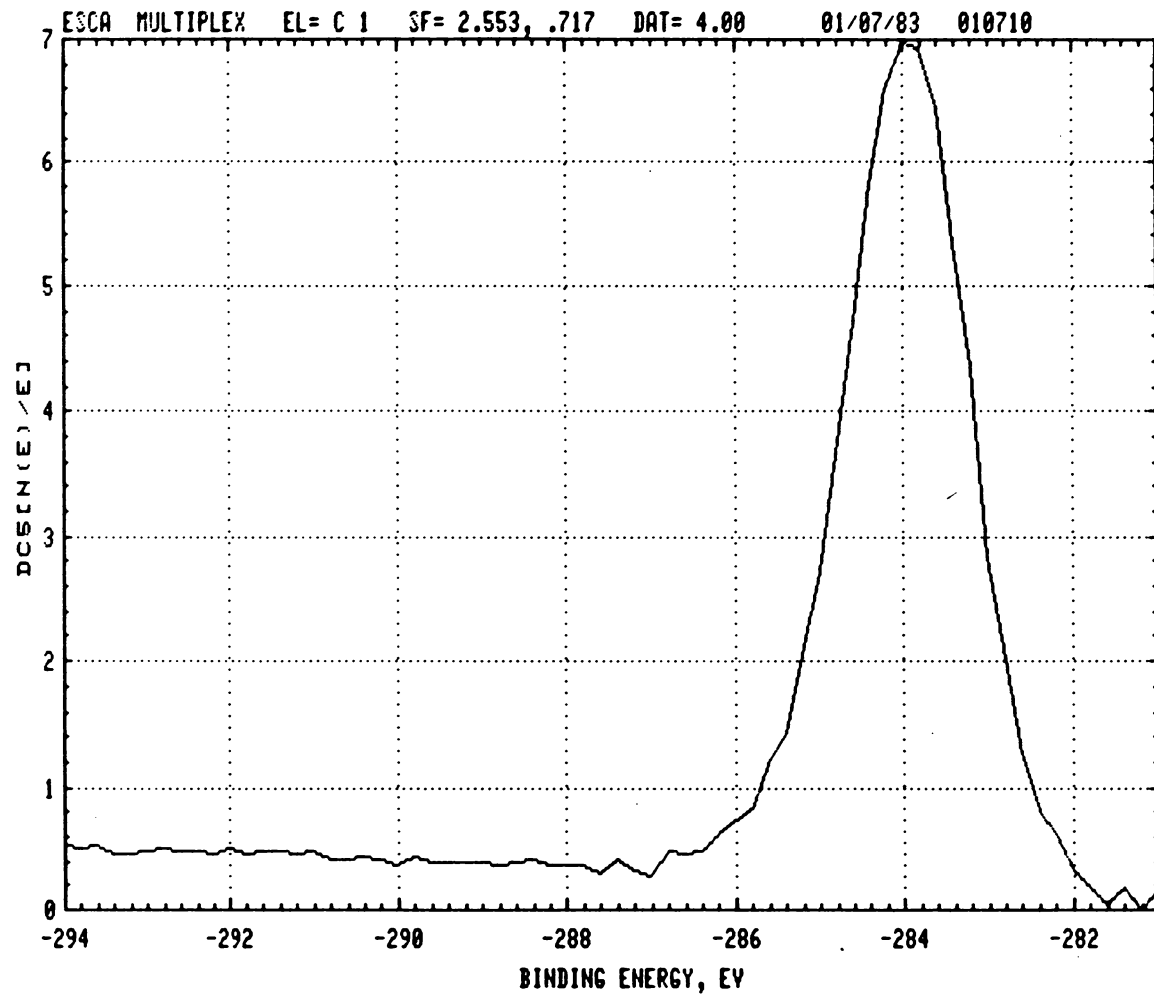


Figure 17. XPS C(1s) Spectrum of Propellant Aged at 75°F for 24 Months

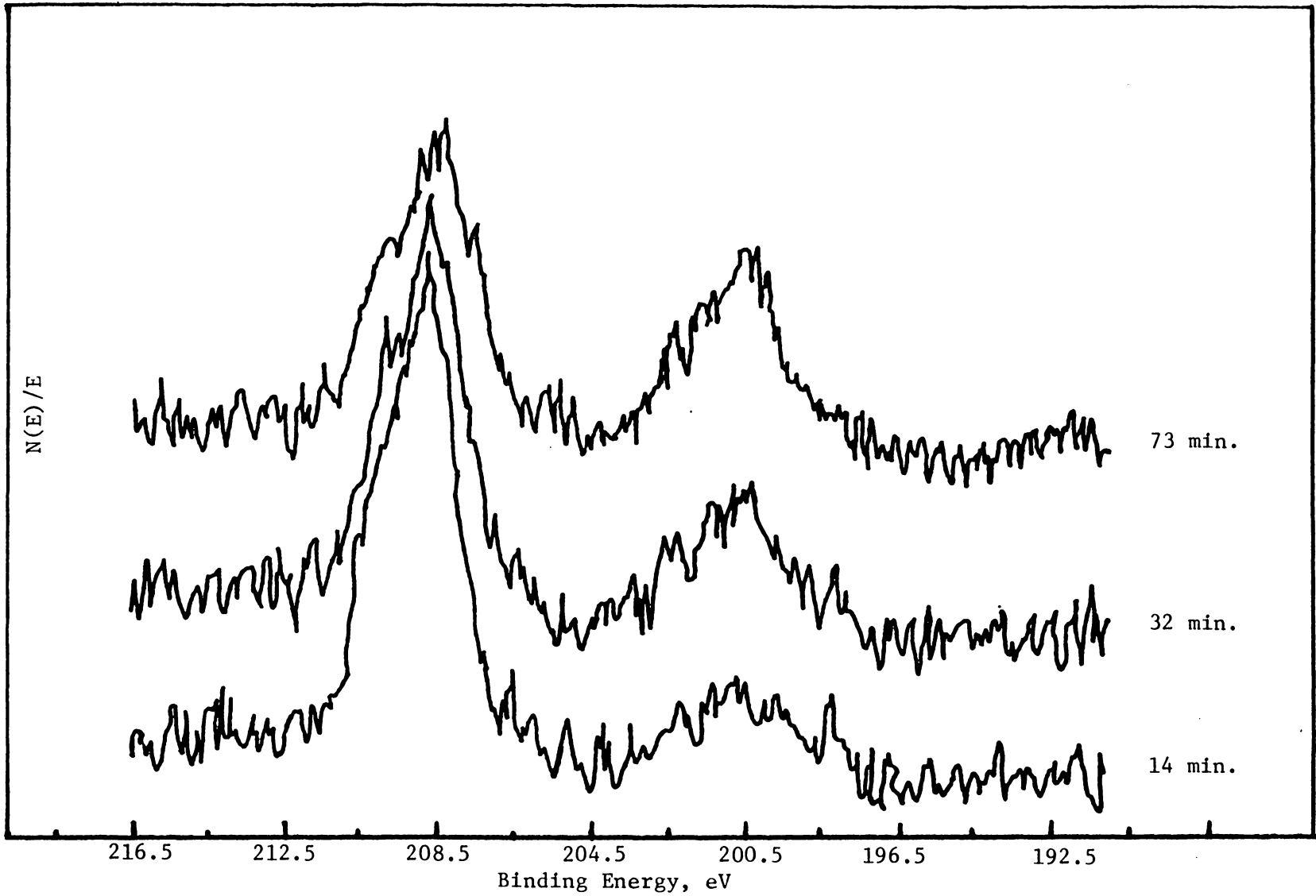


Figure 18. XPS Degradation of Perchlorate in AP

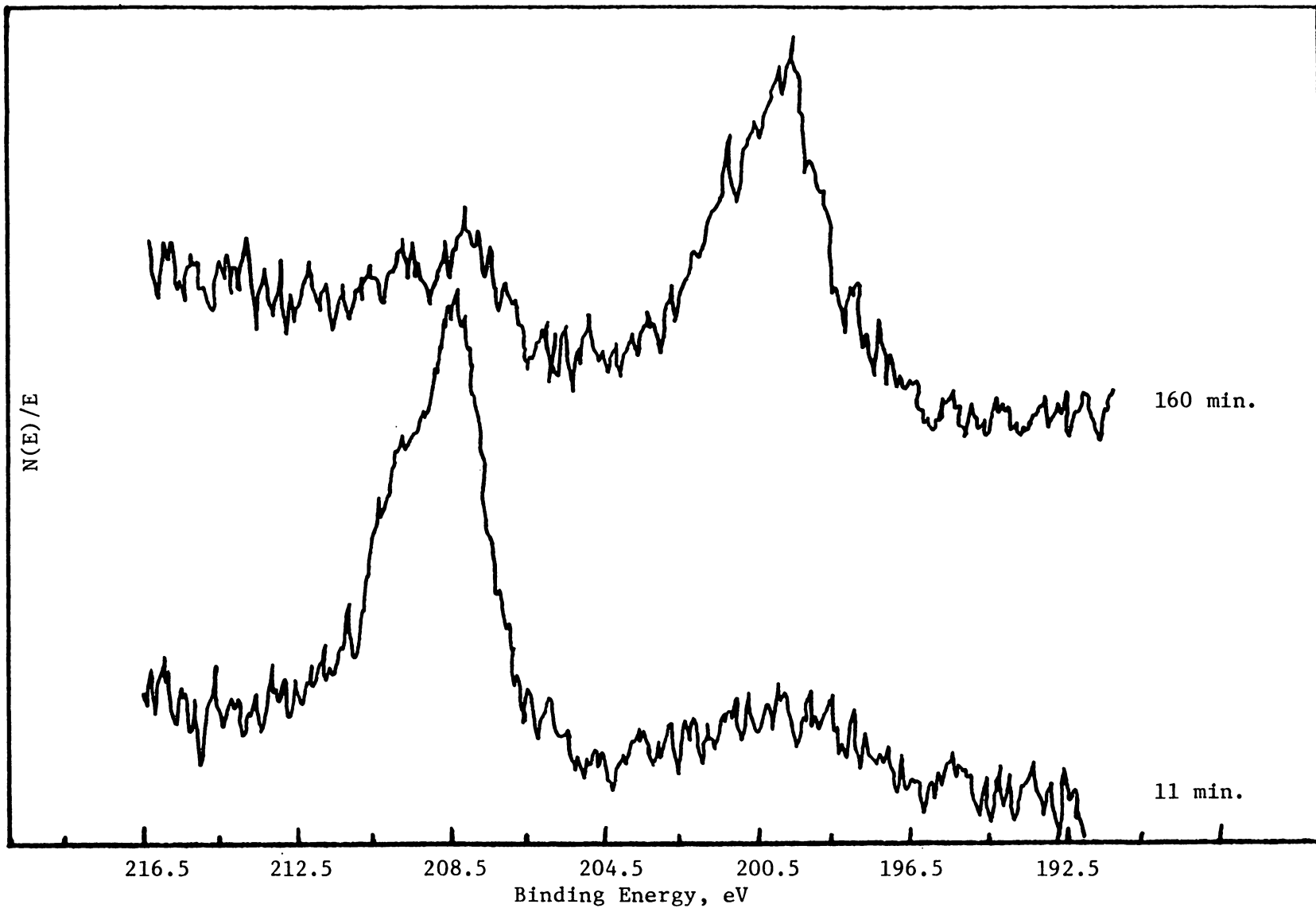


Figure 19. XPS Degradation of Perchlorate in Mix A

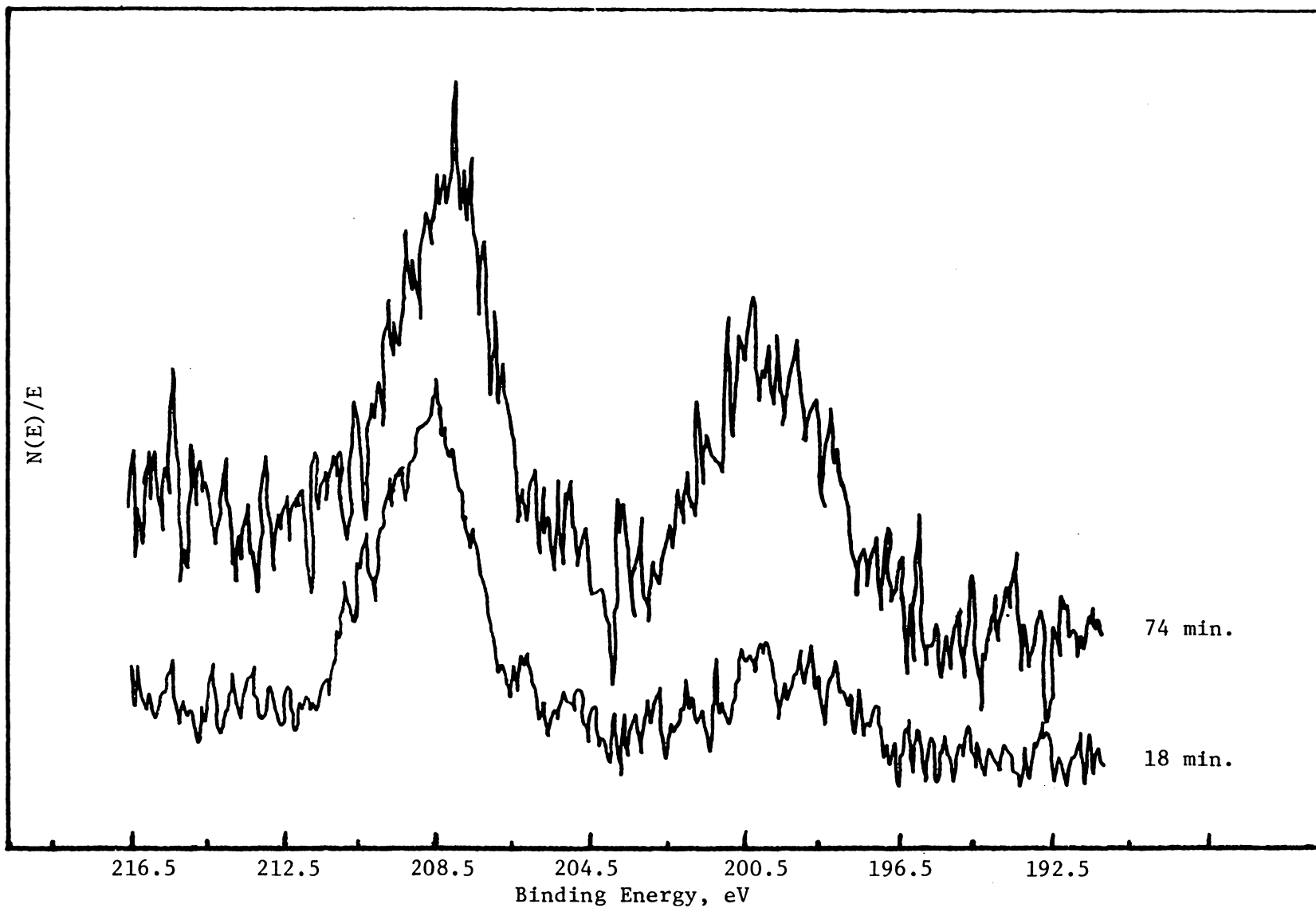


Figure 20. XPS Degradation of Perchlorate in Mix 1

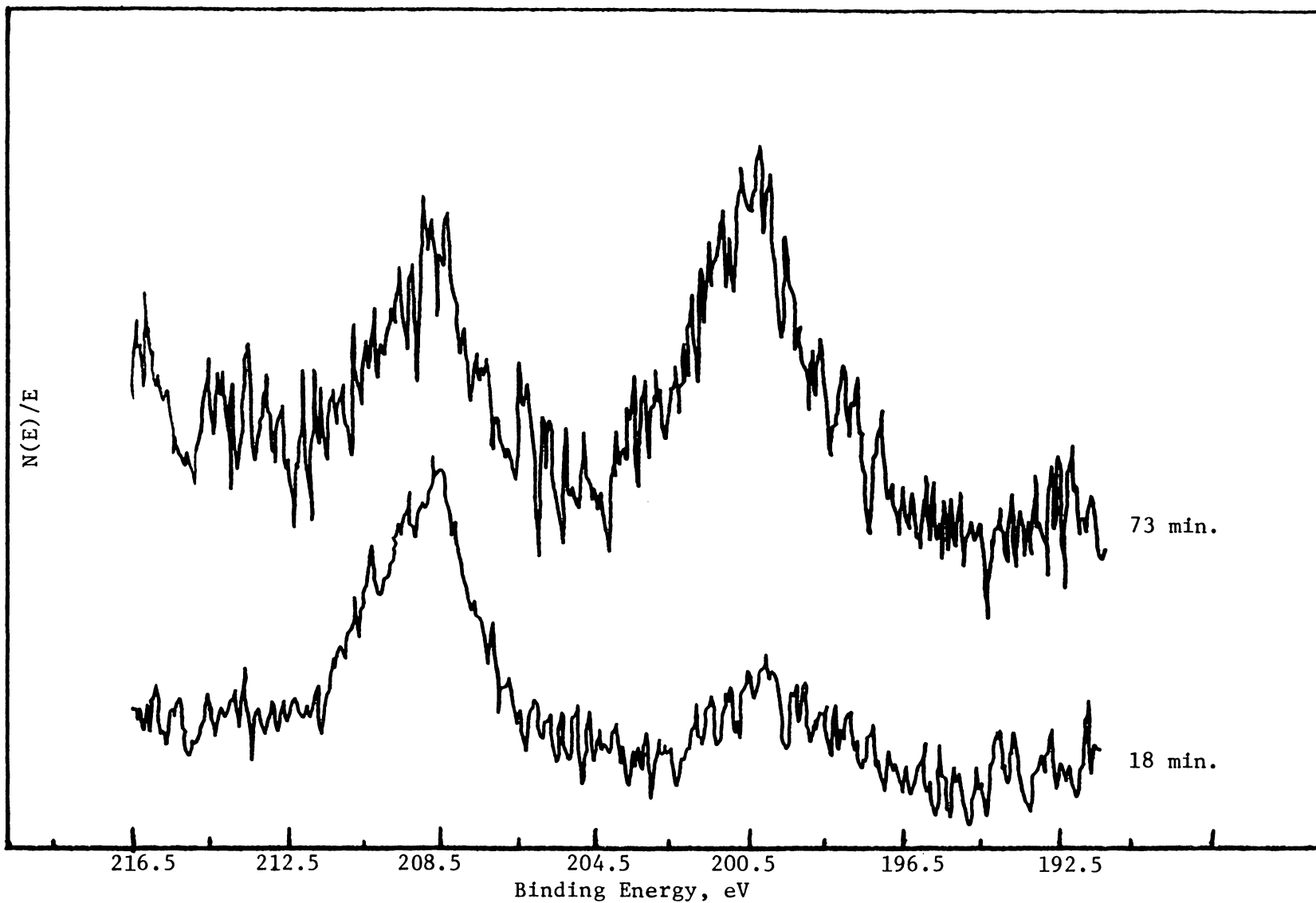


Figure 21. XPS Degradation of Perchlorate in Mix 2

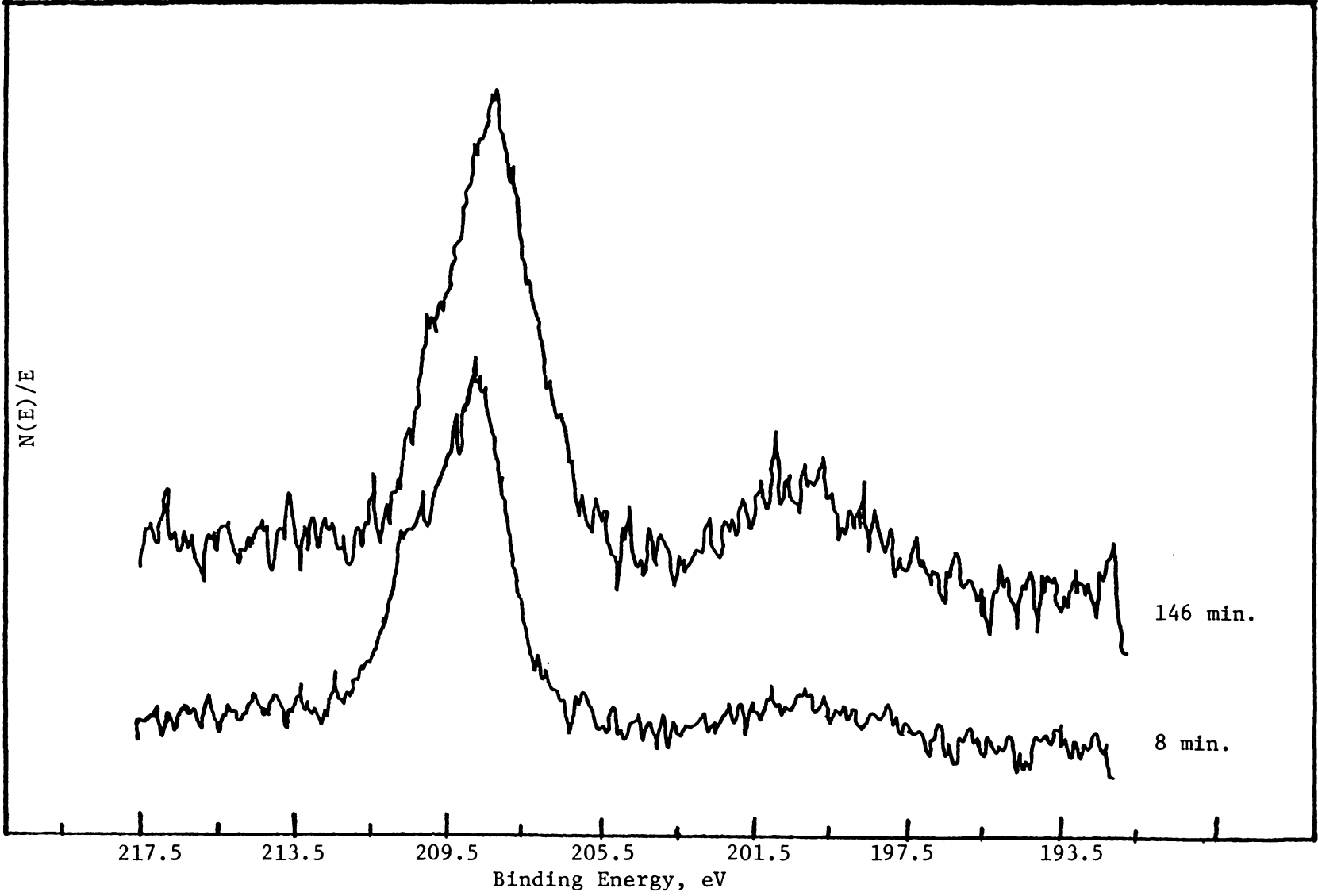


Figure 22. XPS Degradation of Perchlorate in HTPB-AP

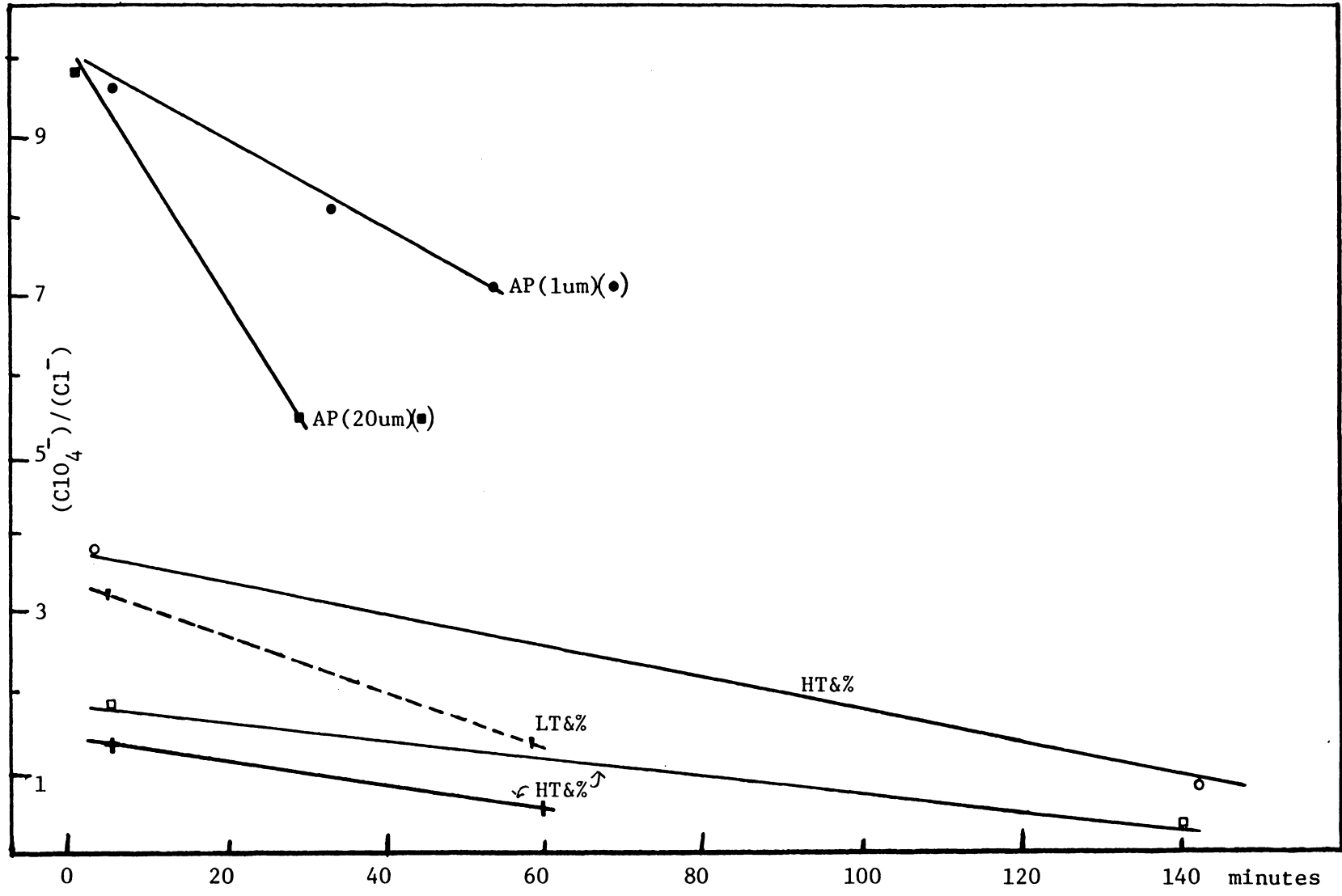


Figure 23. Change in Perchlorate Concentrations under XPS Conditions

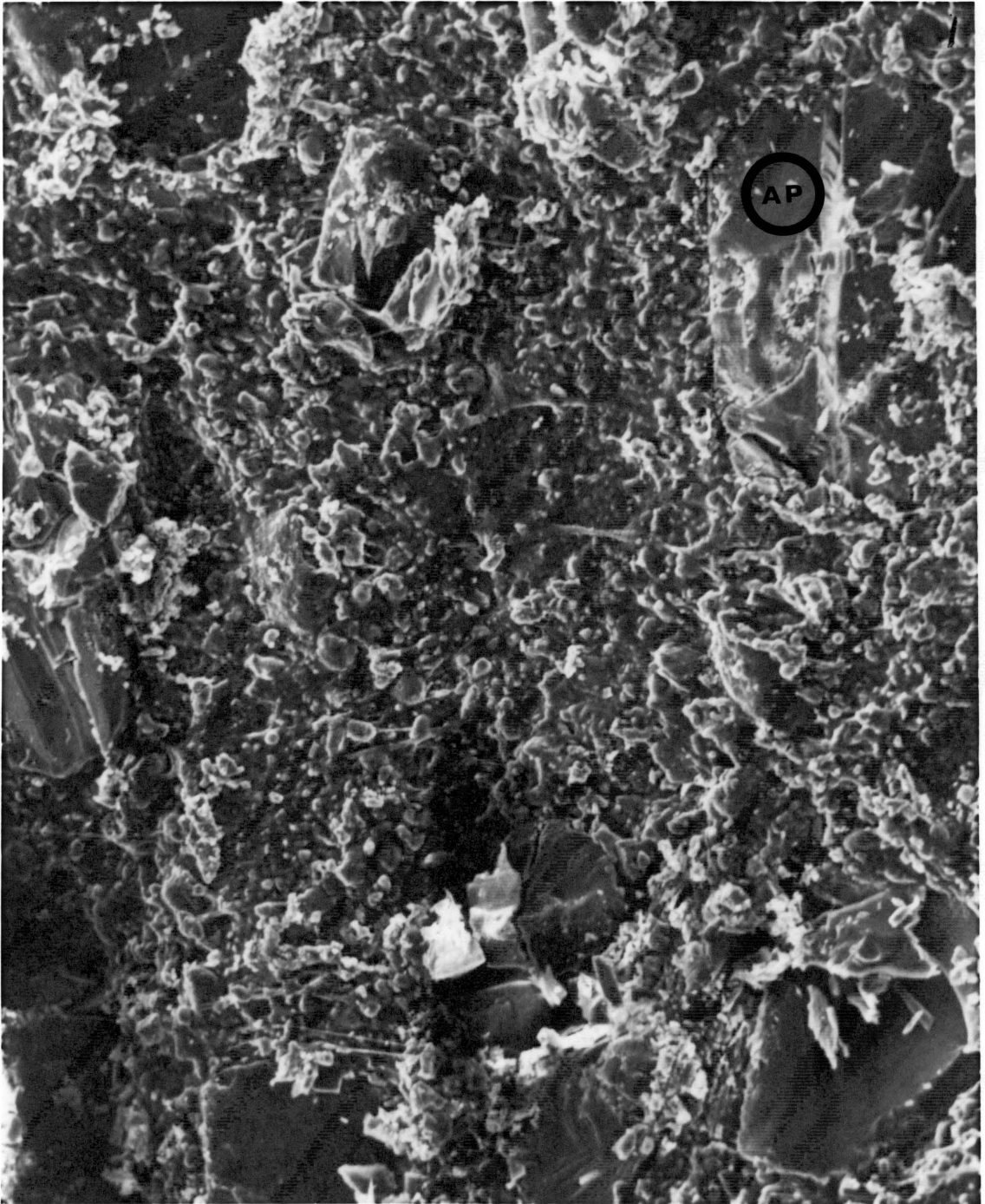


Figure 24. SEM of Unaged Propellant (170X). Scale: 2cm=73um

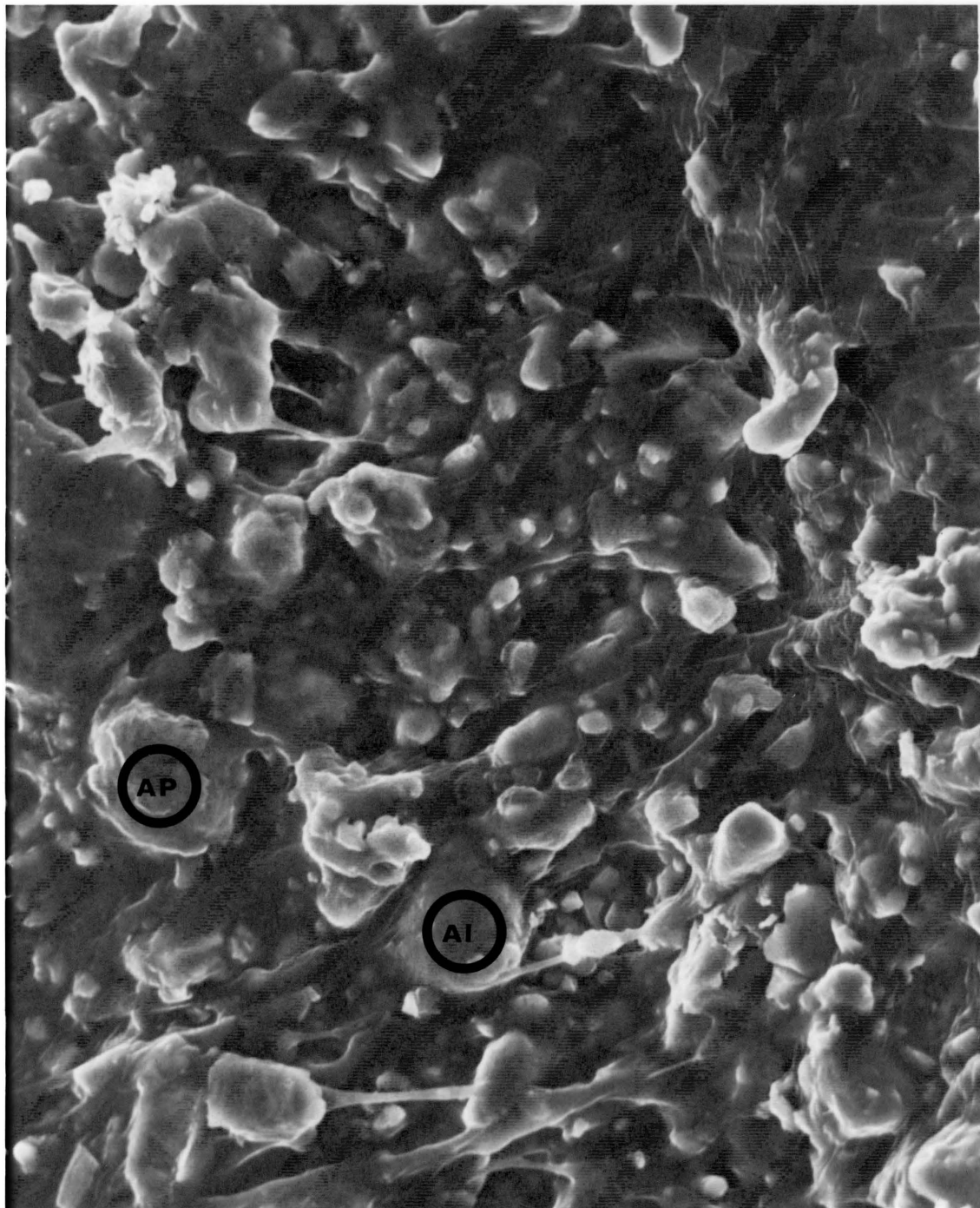


Figure 25. SEM of Unaged Propellant (850X). Scale: 3cm=22um

Pershing propellant. In the 170 photomicrograph, the only discernable features are those due to the 200 μm AP crystals. The slicing operation for sampling purposes appears to cleave these large AP crystals and leaves them exposed on the surface. In the 850x photomicrograph, individual strands of PB are visible, but no small particles are present. It is seen that the 20 μm size Al and AP powders are thoroughly coated with the PB and only EDAX measurements could discern the composition of the nodules. This coating of the small particles indicates that the majority of the AP signal will originate from the 200 μm size particles. The particle coating also indicates why 2 or 4 hour scans were required to pick up a trace Al(2p) photopeak even though it is present at 16-18% by weight. The PB coating is thicker than the electron escape depth for XPS analysis.

Spectral Analysis of N(1s) Photopeak. In Figure 14, the organic N(1s) photopeak is unsymmetrical and this suggests that there are two or more N sources present. One source is the nitrogen in the urethane linkage, while another source could be from any unused IPDI present in the polymer. Due to the noise in the spectra it was not possible to determine whether the minor component disappeared under vacuum and the x-ray flux.

An interesting result that was observed for N(1s) peak in a time degradation experiment is shown in Figure 26. It is seen that either the total amount of "inorganic N" (from AP and NH_4Cl) present is decreasing and/or the amount of "organic N" (from the cured HTPB) is increasing as the sample remains under x-ray flux. Due to the size of

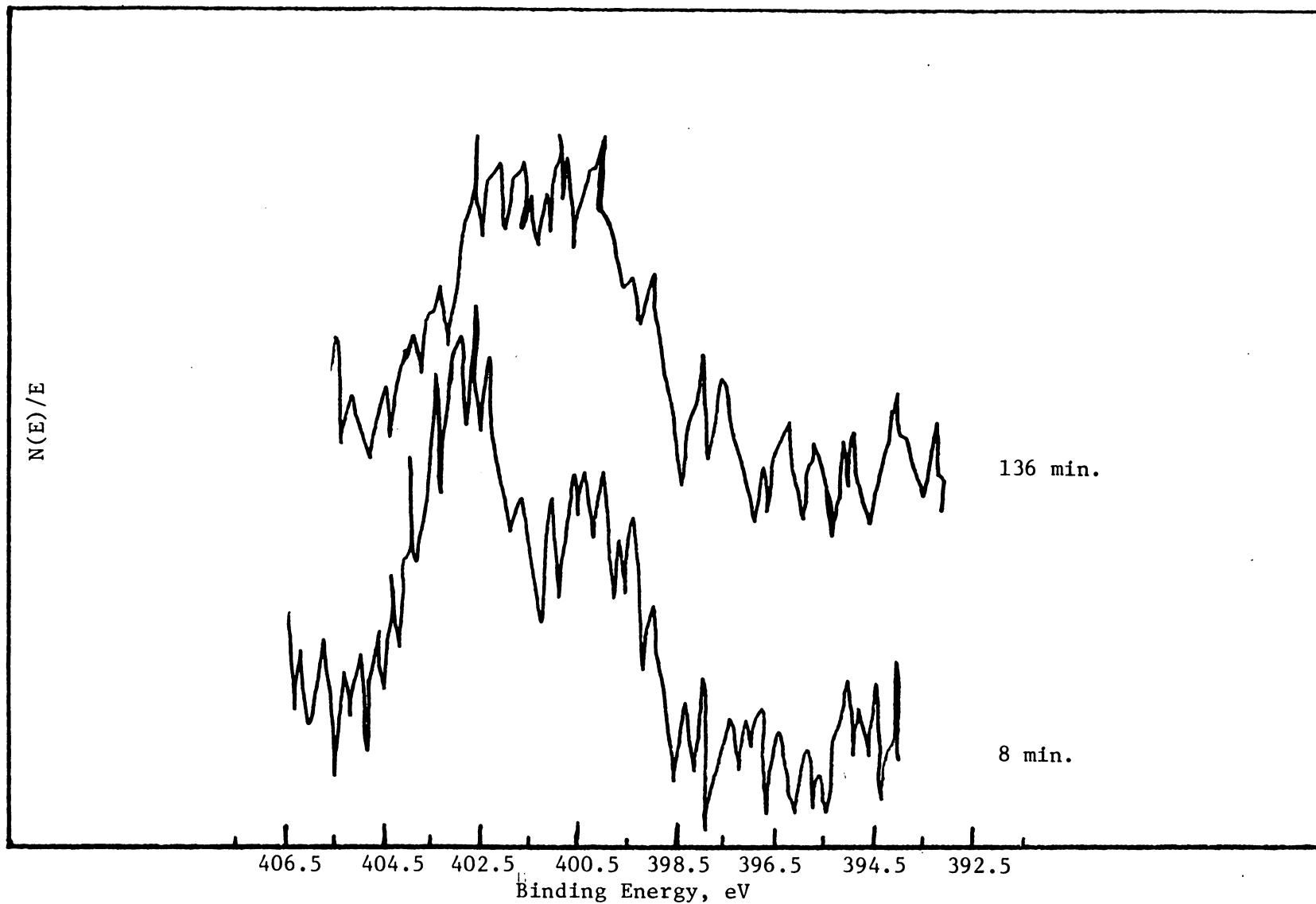


Figure 26. XPS Degradation of N(1s) in Aged Propellant

the AP particles on the sample surface the first assumption by itself is unlikely. A plausible explanation would be that some of the AP is degrading and then that the one product, NH_3 , cleaves the urethane linkage and is added onto the polymer end group. This explanation allows for the inorganic N to decrease and the amount of organic N to increase.

With this assumption the interpretation of Figures 27 through 31, for various samples stored at low and high temperature conditions, is made easier. All the spectra show an increase in the organic N content when going from the low to high temperatures. This seems reasonable as AP is expected to degrade faster at higher temperatures thus increasing the likelihood of the urethane cleavage to occur. When no AP is present in the HTPB there was no change in the organic N content between the different ageing temperatures. This can be seen in Figure 32 for the HTPB-Al mixture where both the low and high temperature curves are identical (only the unaged sample is shown).

Even though there is an apparent increase in the amount of organic N present at the higher ageing conditions, over a period of time the inorganic/organic N ratio decreases for most samples. This could be due to a loss of unused IPDI. This should not account for such losses, yet no other plausible reason is available. These losses are shown in Figure 33 and 34. The lower rate of loss for the aged sample (Ht&%) runs could be caused by the urethane cleavage run slowing the apparent rate of organic N loss. Two samples, Mix 1 and Mix 2, might show the opposite trend, an increase of organic N with time, and this could

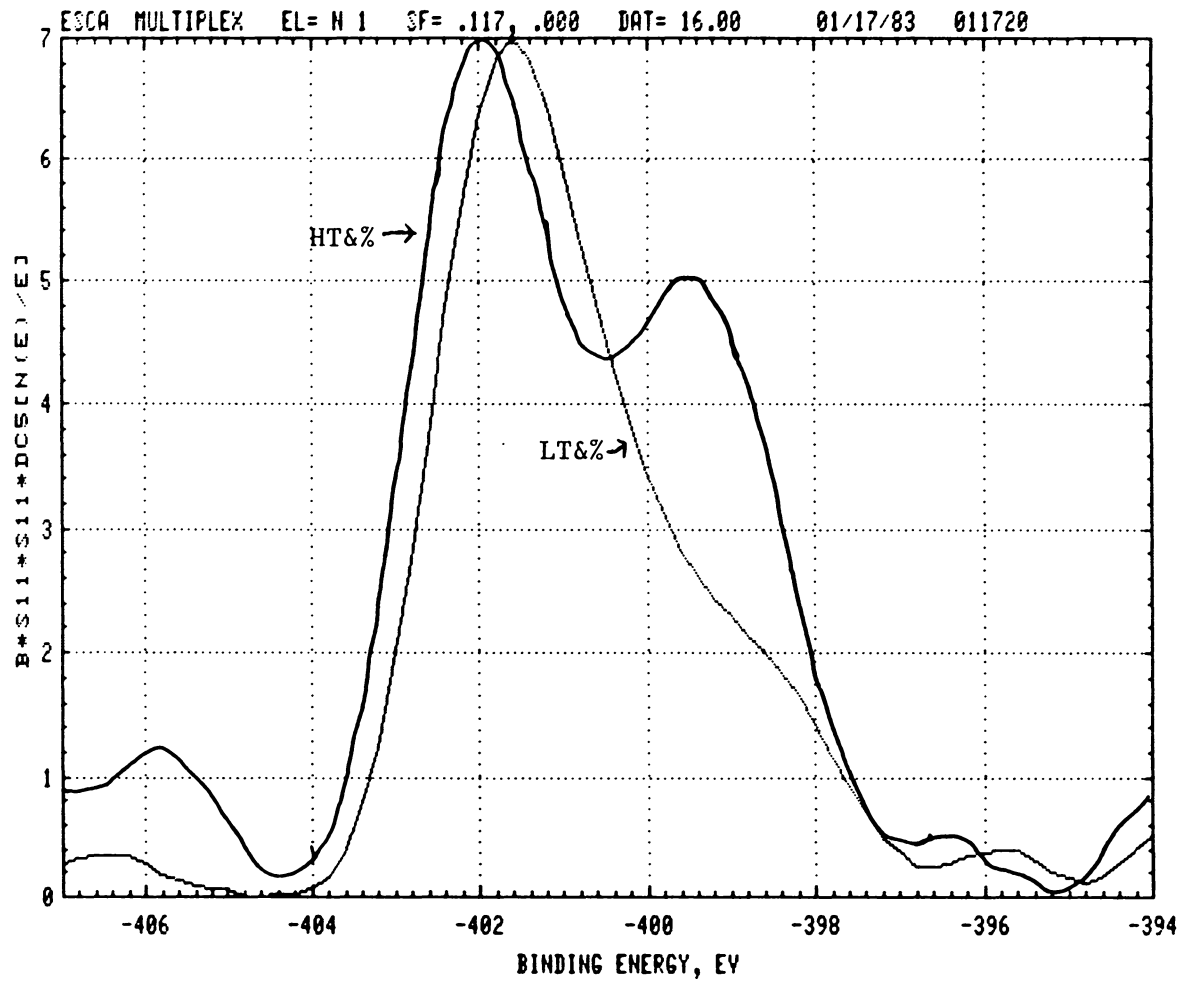


Figure 27. Change in N(1s) Source for Mix 1

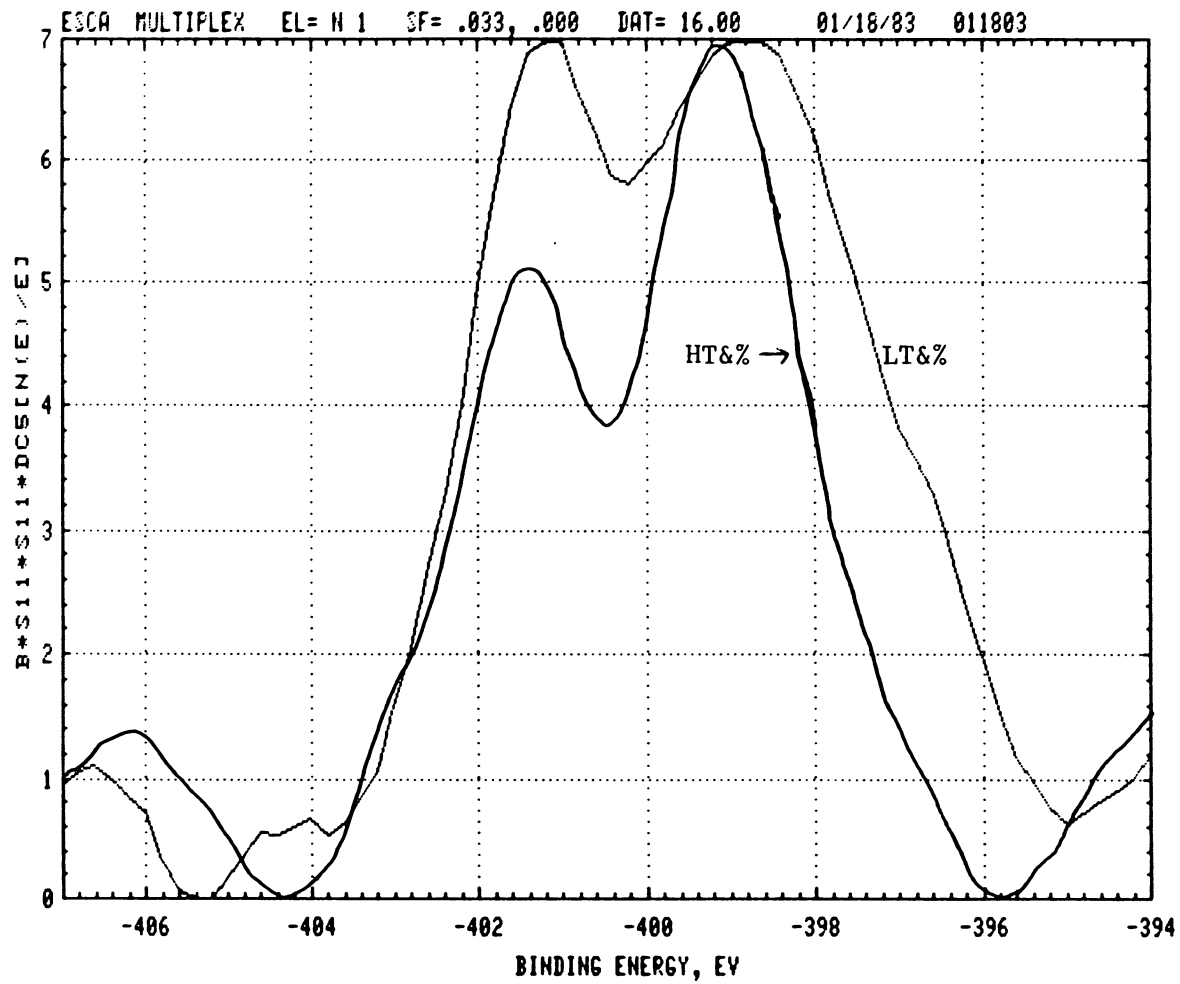


Figure 28. Change in N(1s) Source for Mix 2

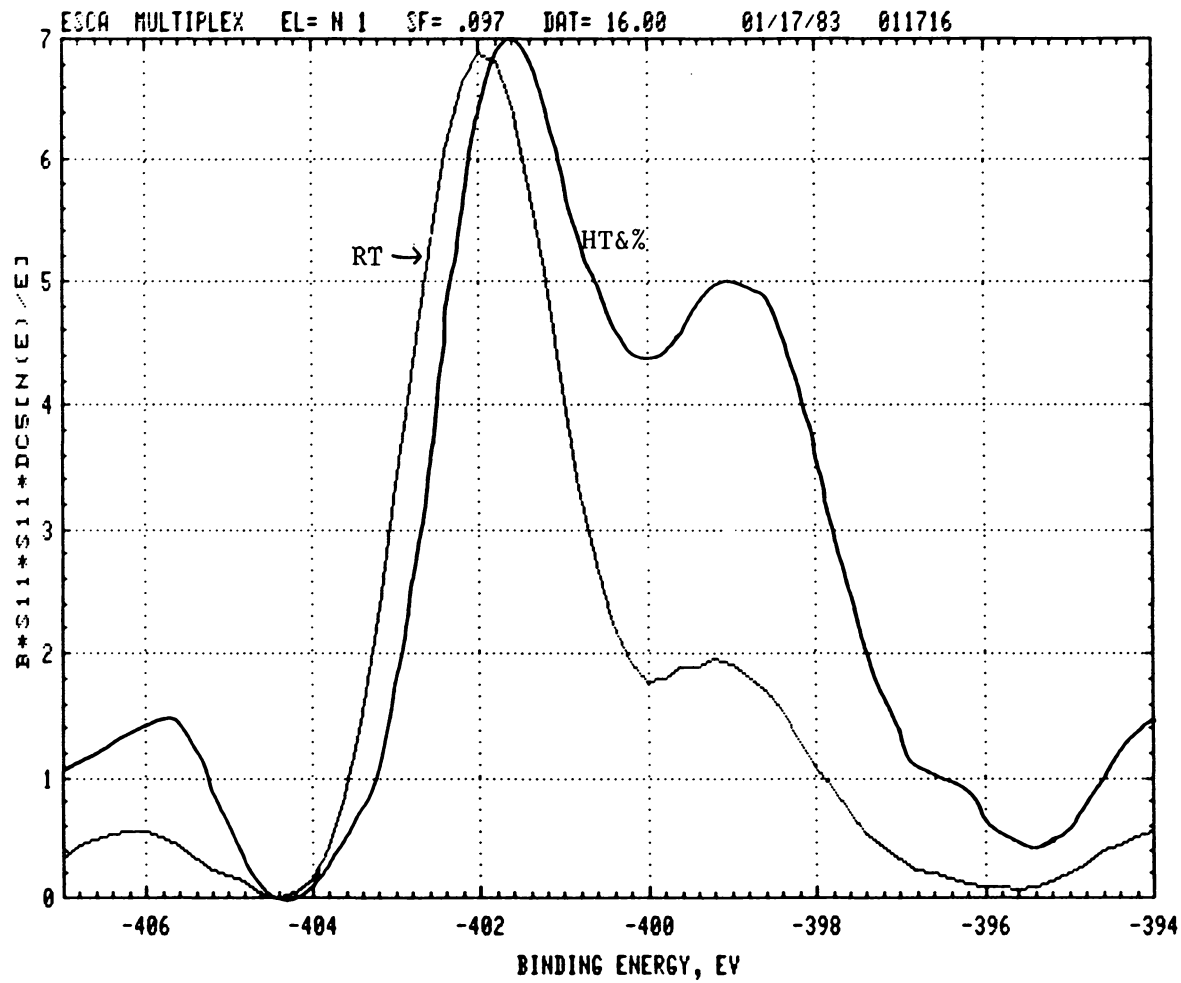


Figure 29. Change in N(1s) Source for Sample VIII

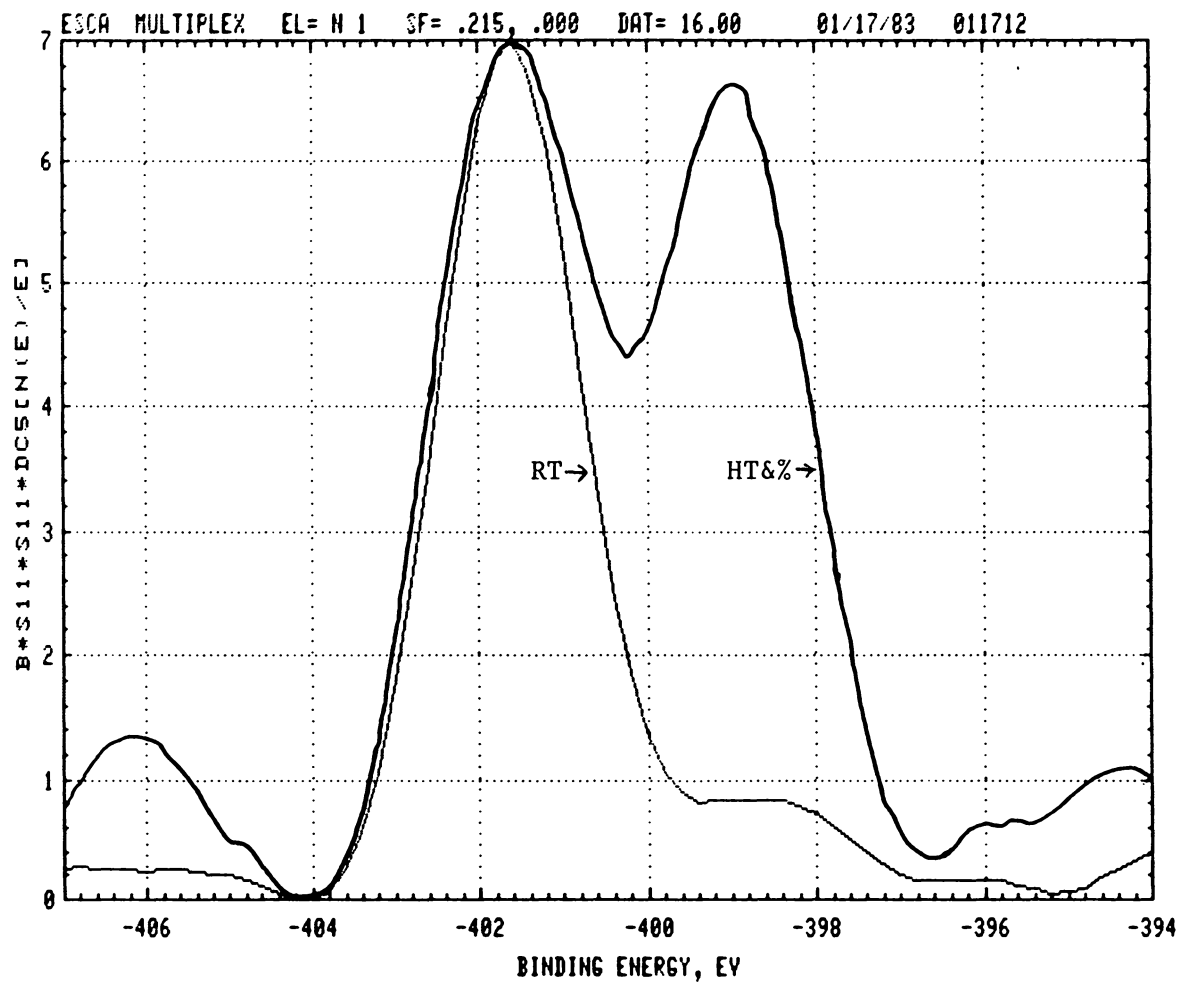


Figure 30. Change in N(1s) Source for Sample VII

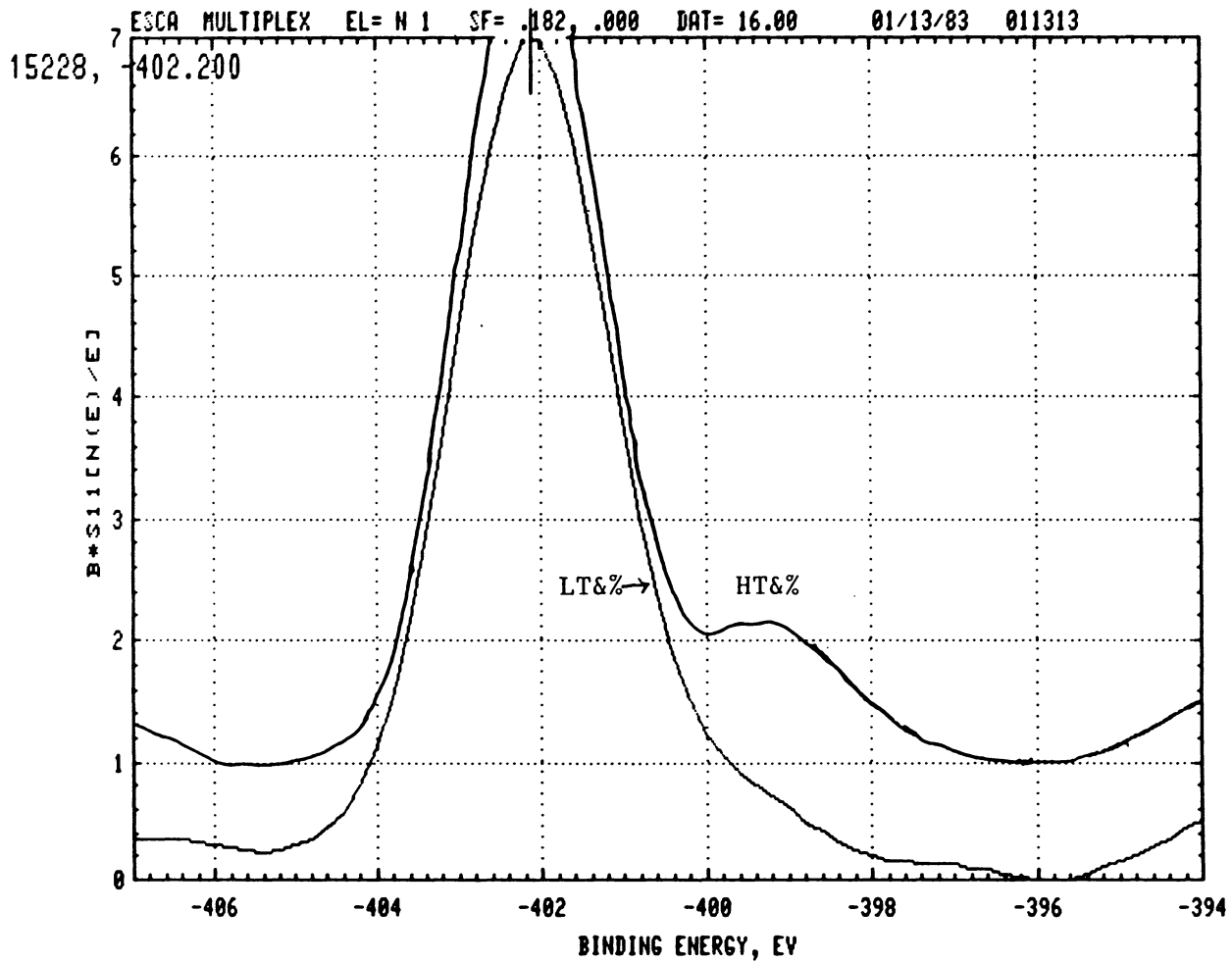


Figure 31. Change in N(1s) Source for Mix A

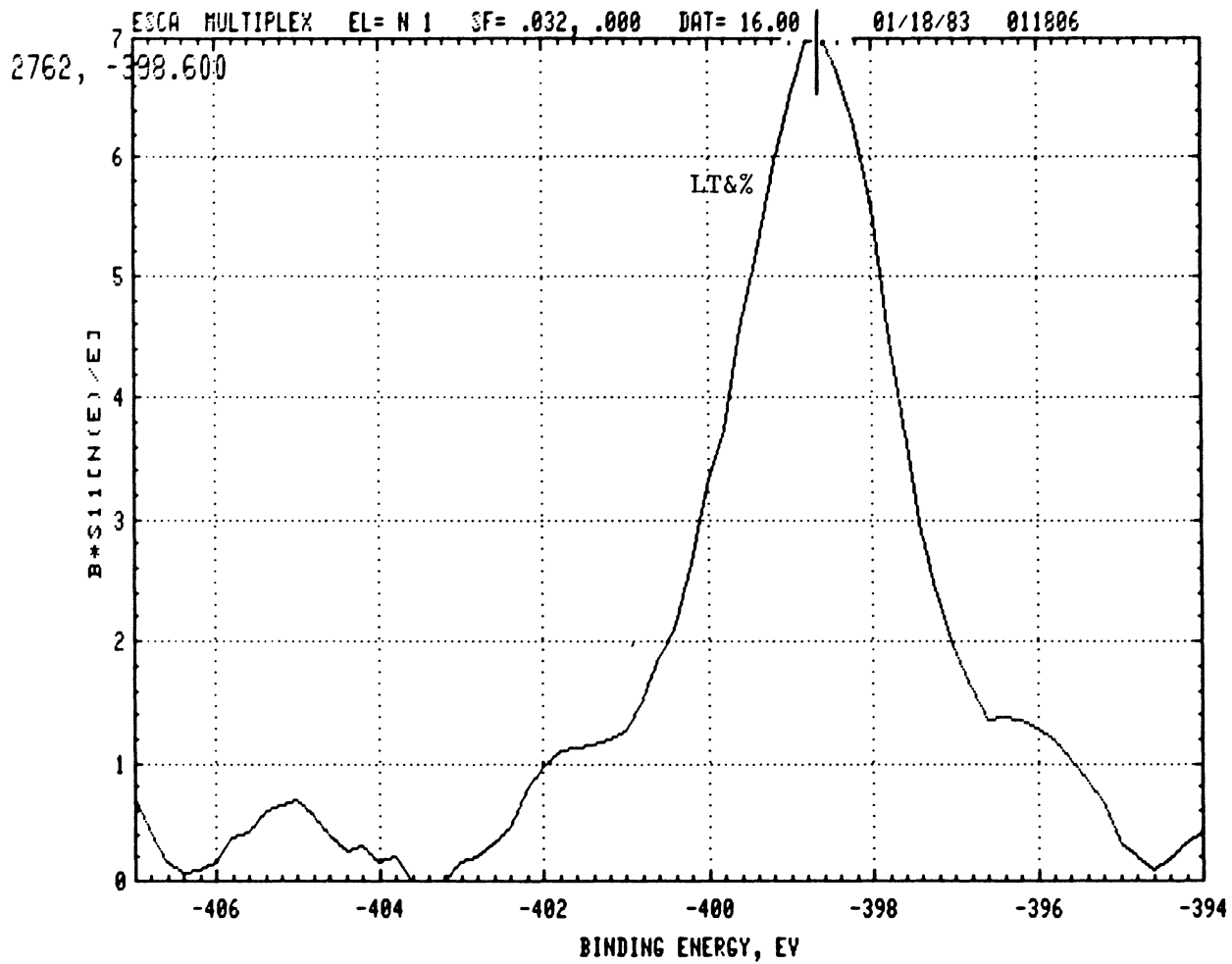


Figure 32. Change in N(1s) Source for Mix 3

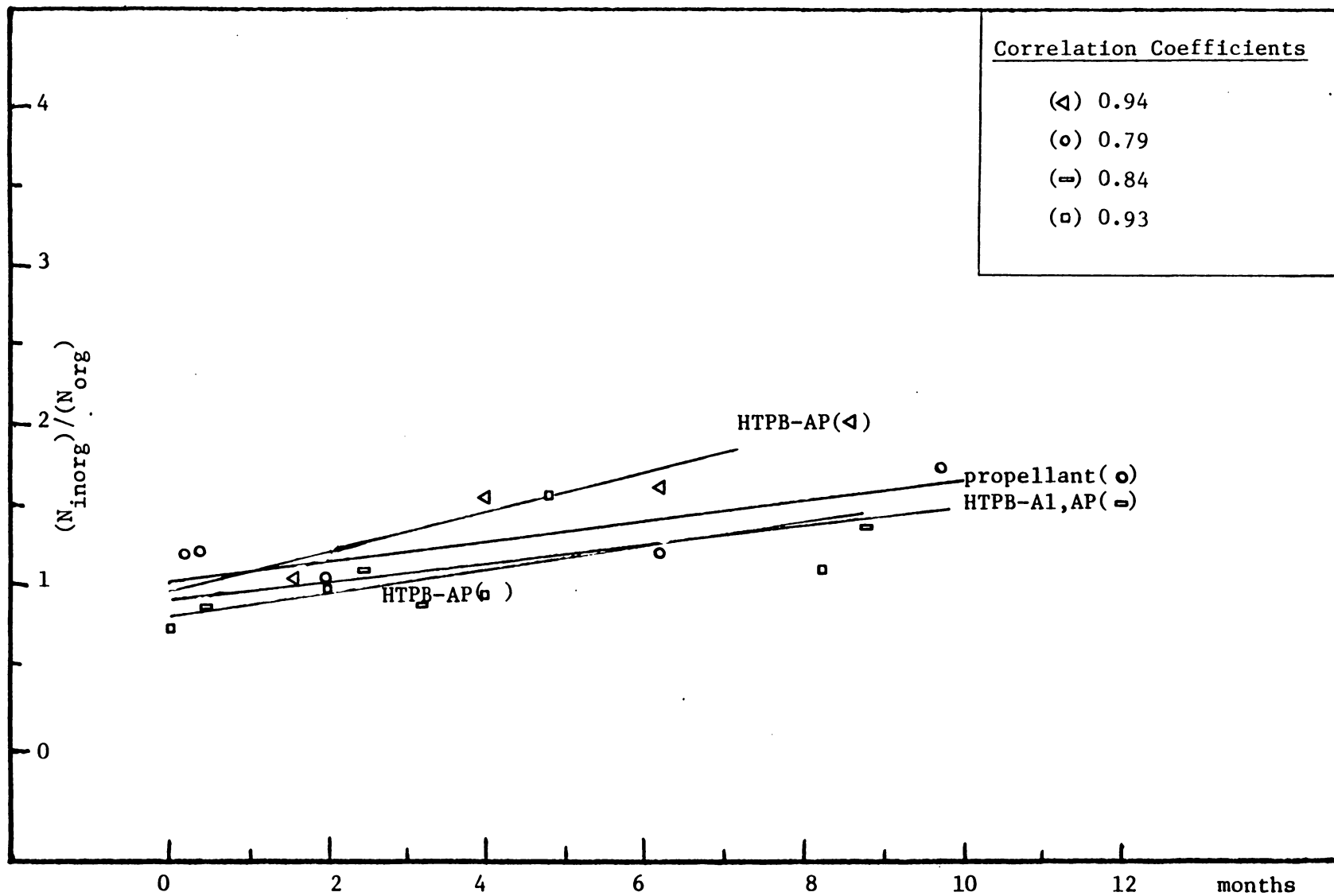


Figure 33. Change in N(1s) Source for Samples Aged at HT&% Overtime

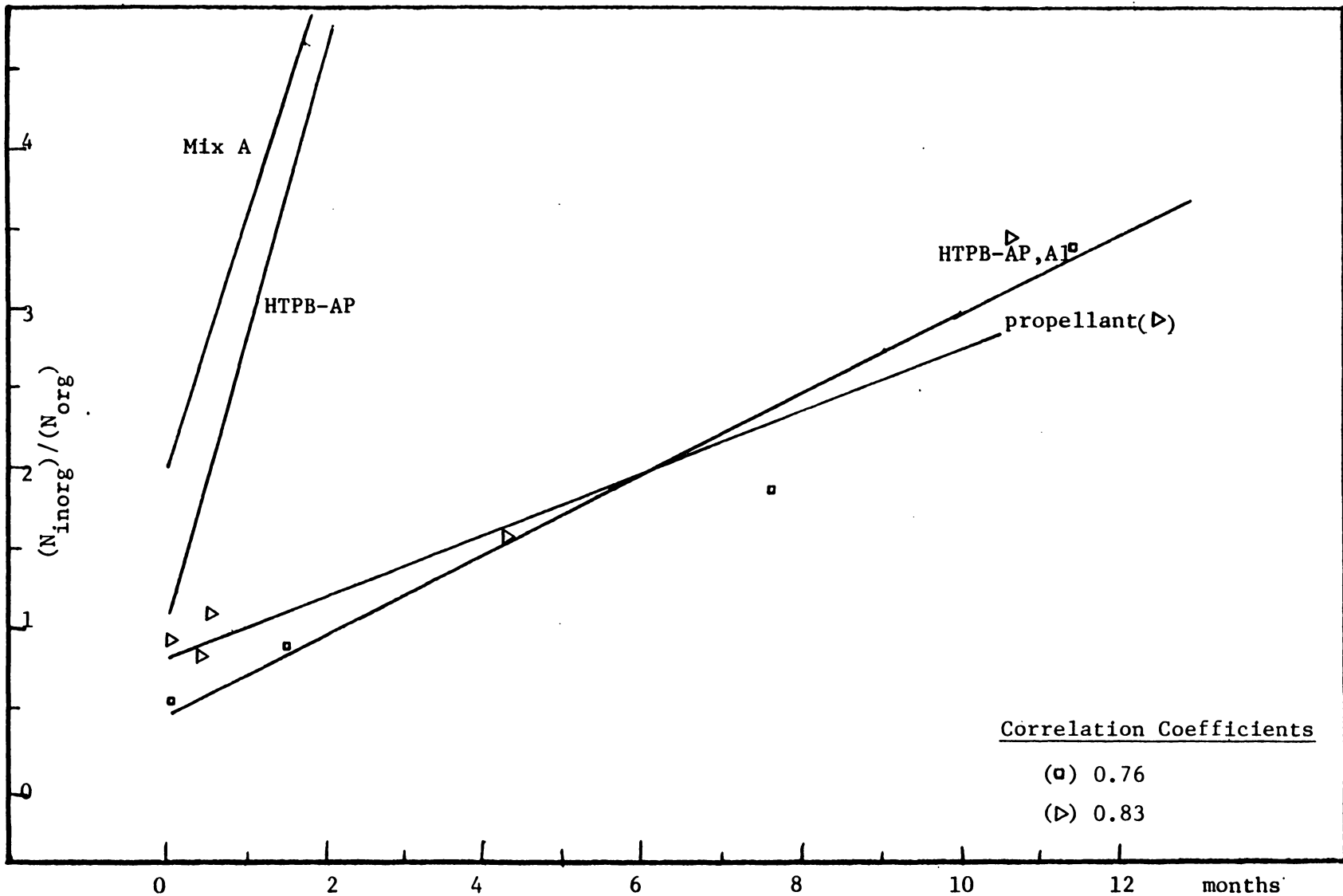


Figure 34. Change in N(1s) Source for Sample Aged at LT&% Overtime

be explained by the fact that the small AP therefore seeing a smaller amount of them on the surface of the sample. A longer study period for Mix 1 and 2 would be needed to see if this opposite trend is real.

Spectral Analysts of Cl(2p) Photopeak. The main thrust of the XPS study was directed at monitoring the loss of ClO_4^- , due to the ageing process, by monitoring the Cl(2p) peak. The relative intensities of the Cl^{+7} and Cl^- photopeaks were observed for compositional changes in the sample. A problem arose in that the Cl(2p) photopeak from NH_4Cl partially overlapped with the x-ray satellite peaks from the Cl^{+7} photopeak. It was difficult to determine how much the Cl^- photopeak contributed to the baseline hump in the unaged samples without deconvolution technique.

The amount of Cl^- present in a propellant increases between the unaged and aged samples. This is shown in Figures 35 through 39 for various samples. For a "fresh" propellant, Mix A, there was no discernable difference between the unaged and aged samples after a 6 month period. Figure 40 shows that there is some Cl^- present in these samples but not much. The exception to this is Mix 2, shown in Figure 41, in which there is a decrease in Cl^- concentration between the ageing conditions.

The loss of Cl^- over time is shown in Figure 42. Due to wide scattering of the experimental ratios, in many samples there were no visible trends. For the samples shown the loss of NH_4Cl overtime is faster for aged samples at HT&% than for unaged samples. Though more NH_4Cl may be formed at higher temperatures it is also lost more

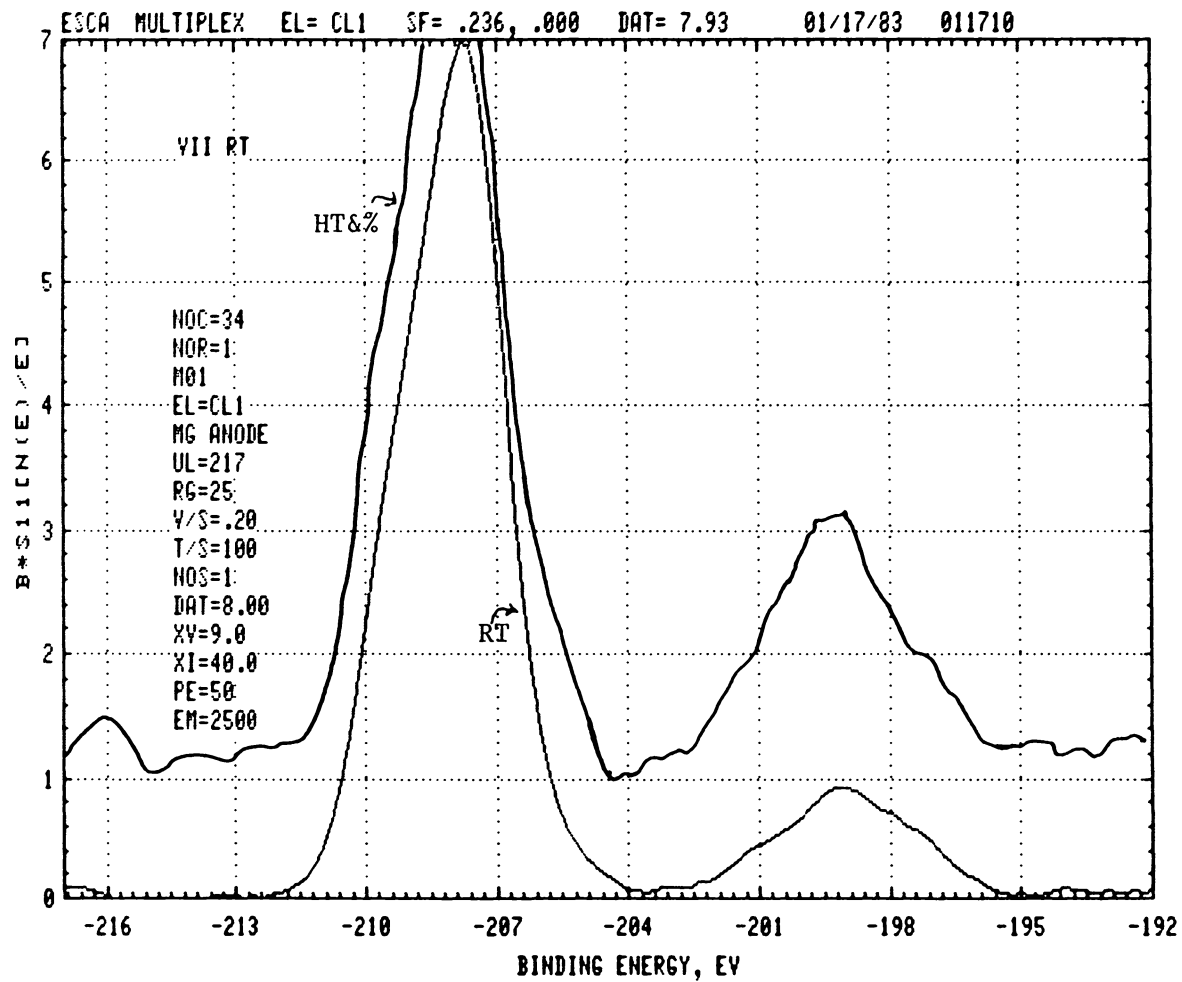


Figure 35. Cl^- Concentration Changes Between Ageing Conditions for Sample VII

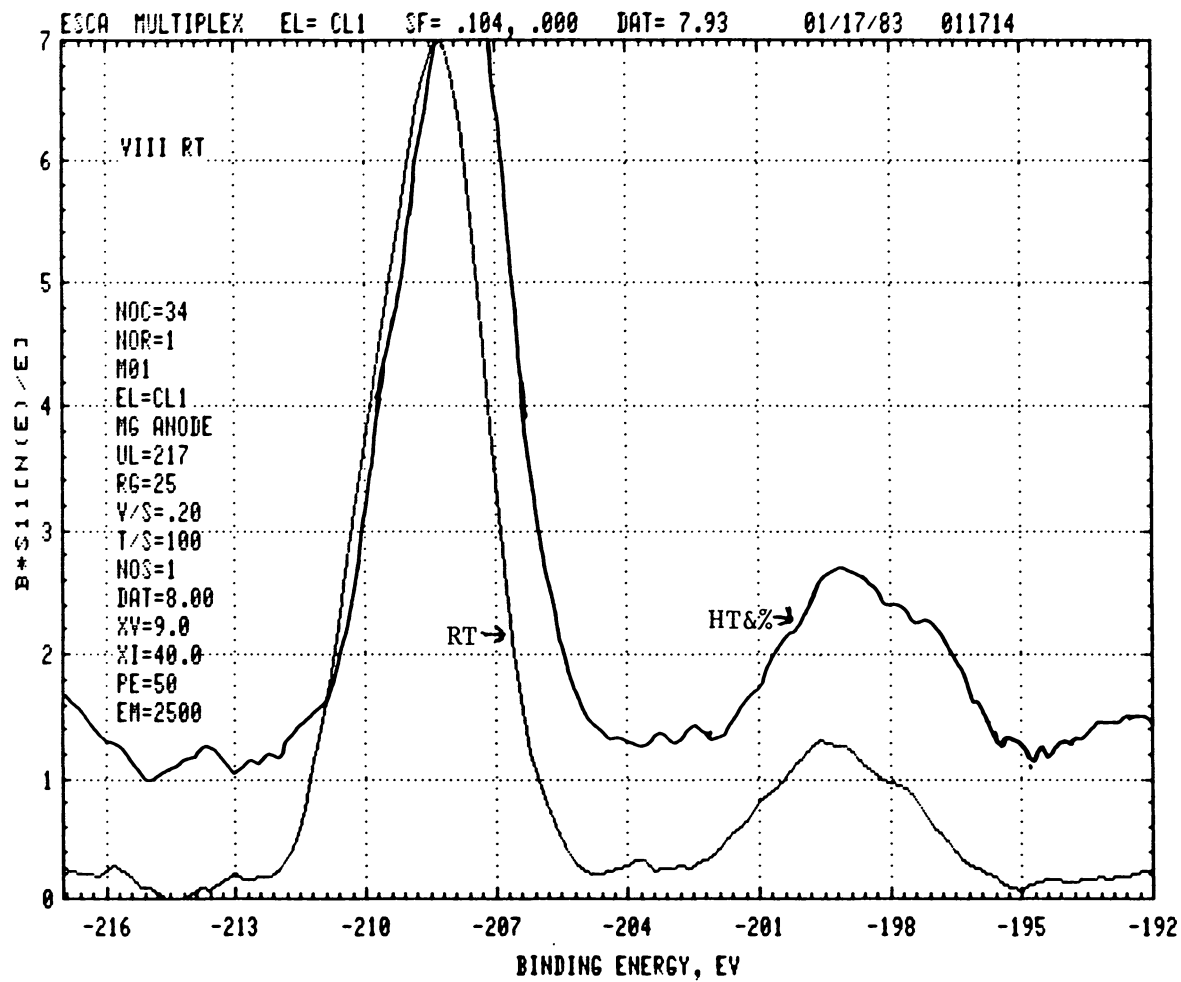


Figure 36. Cl^- Concentration Changes Between Ageing Conditions for Sample VIII

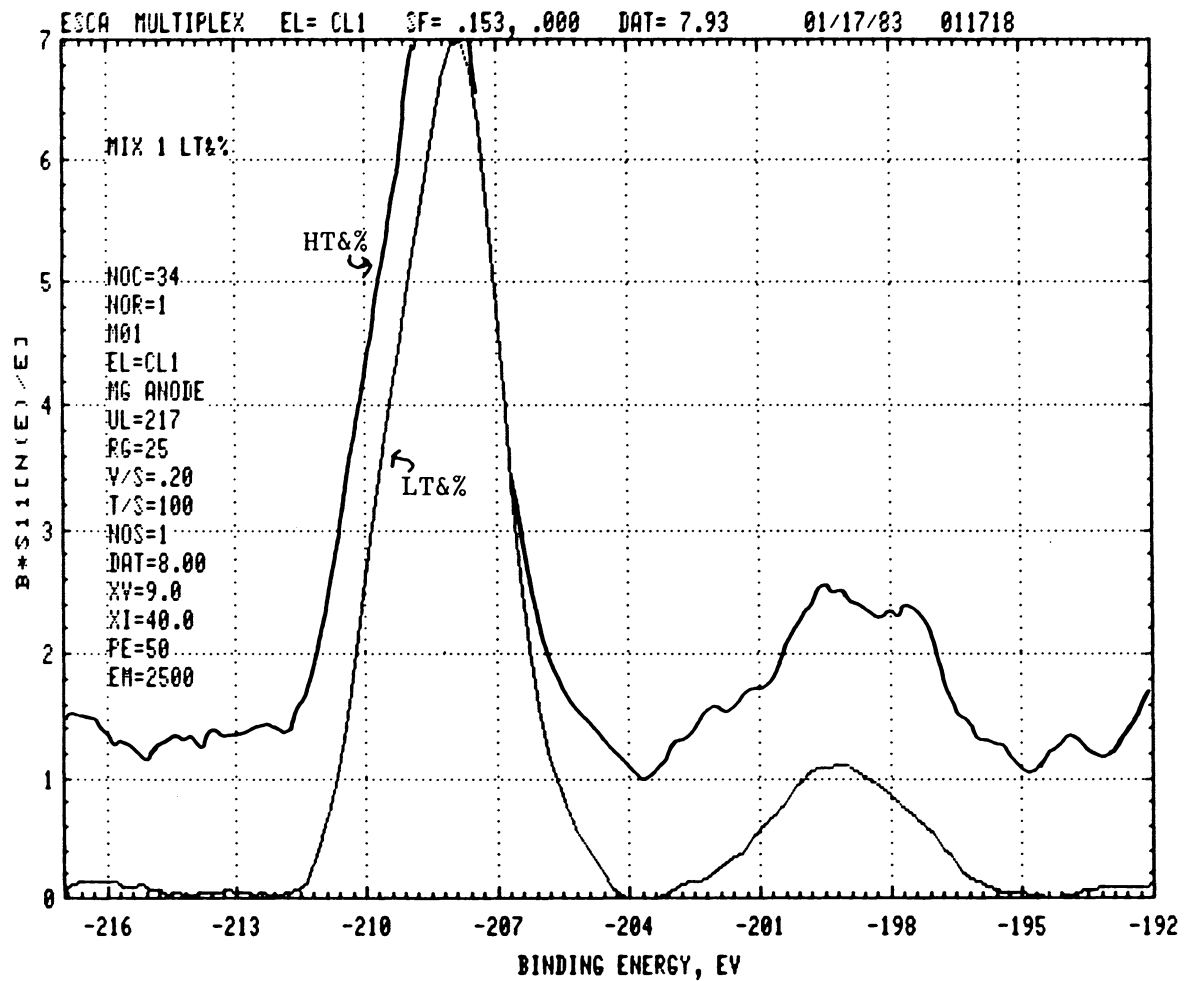


Figure 37. Cl^- Concentration Changes Between Ageing Conditions for Mix 1

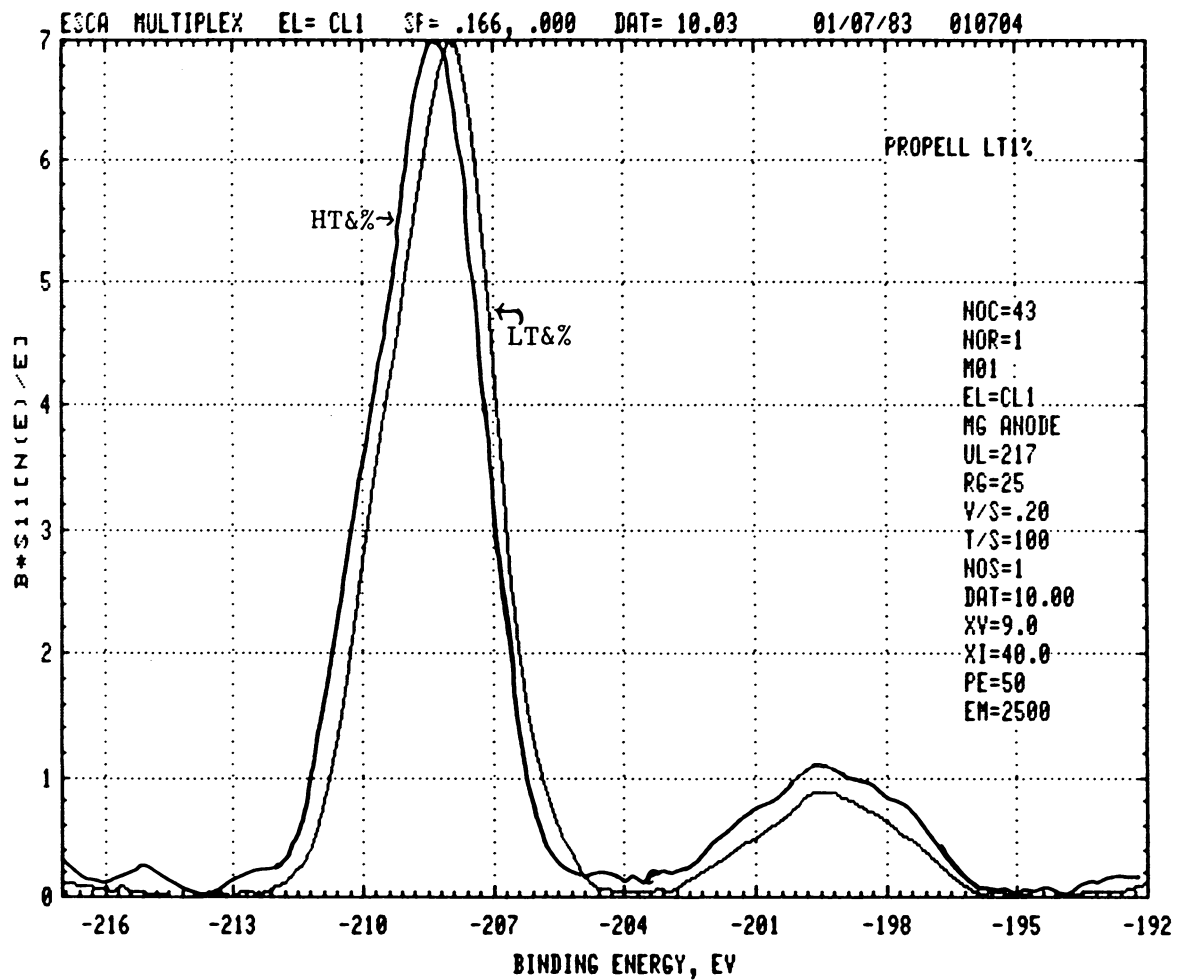


Figure 38. Cl^- Concentration Changes Between Propellant Ageing Conditions

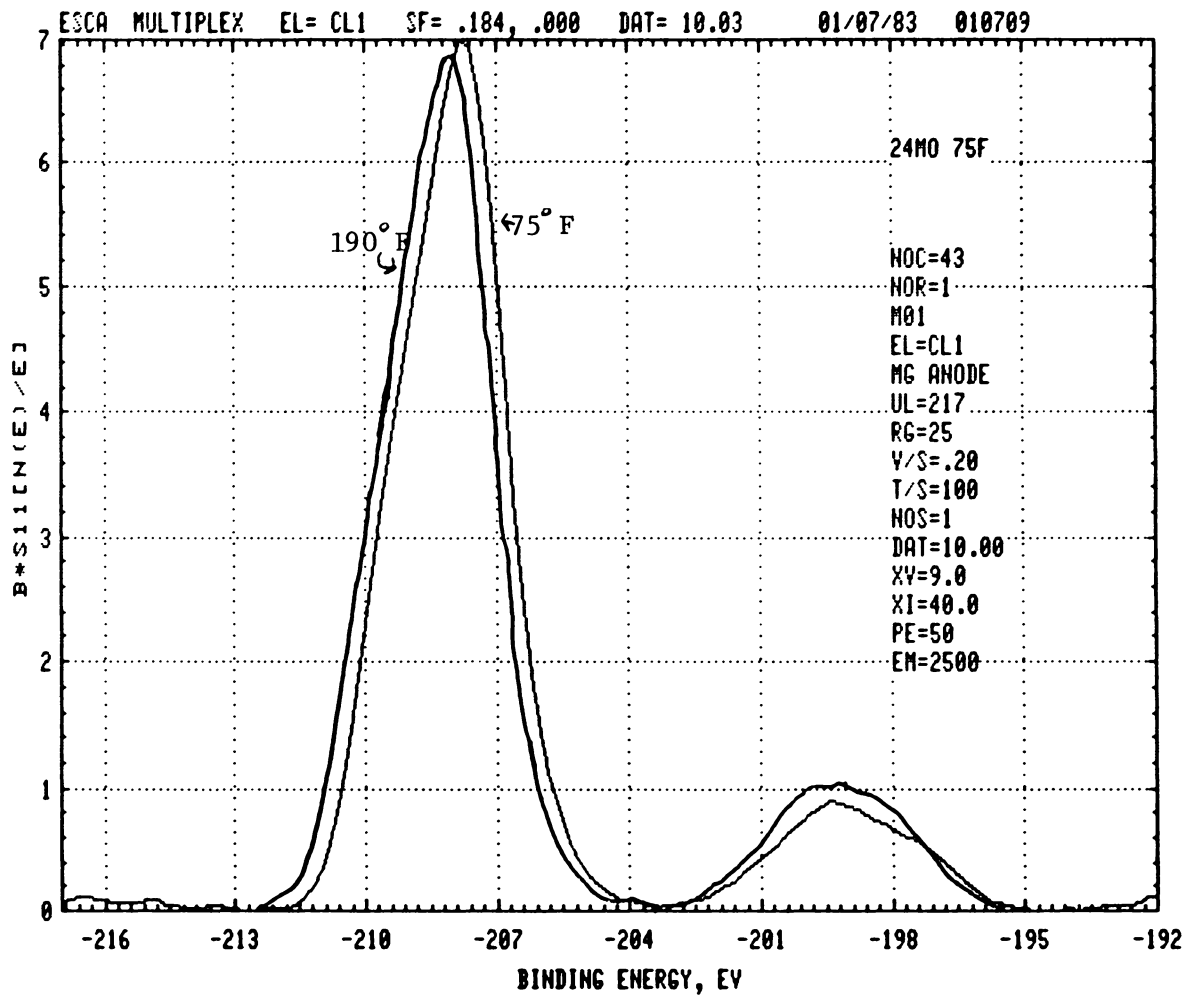


Figure 39. Cl^- Concentration Changes Between Propellant Longterm Ageing Conditions

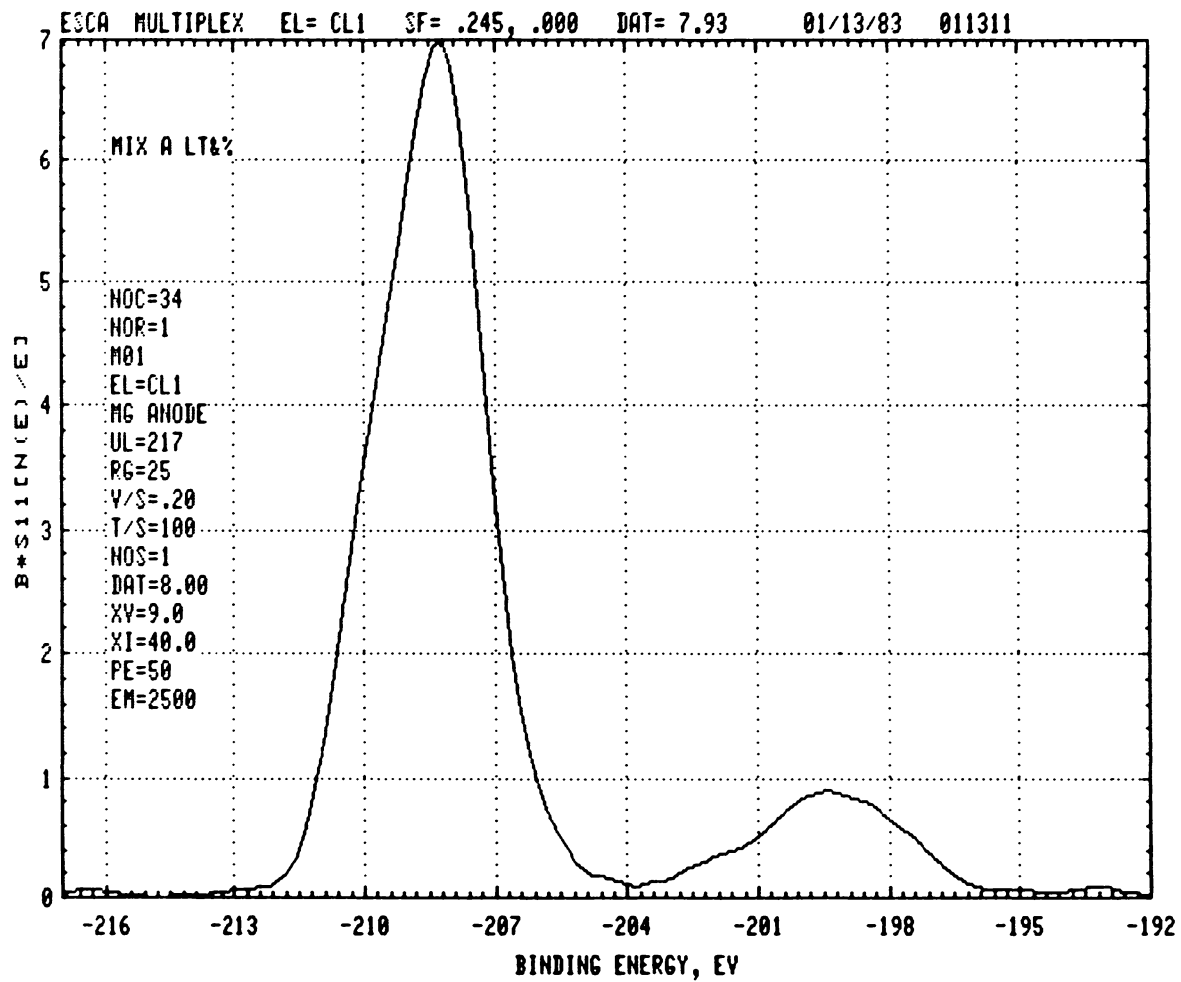


Figure 40. Cl^- Concentration Changes Between Mix A Ageing Conditions

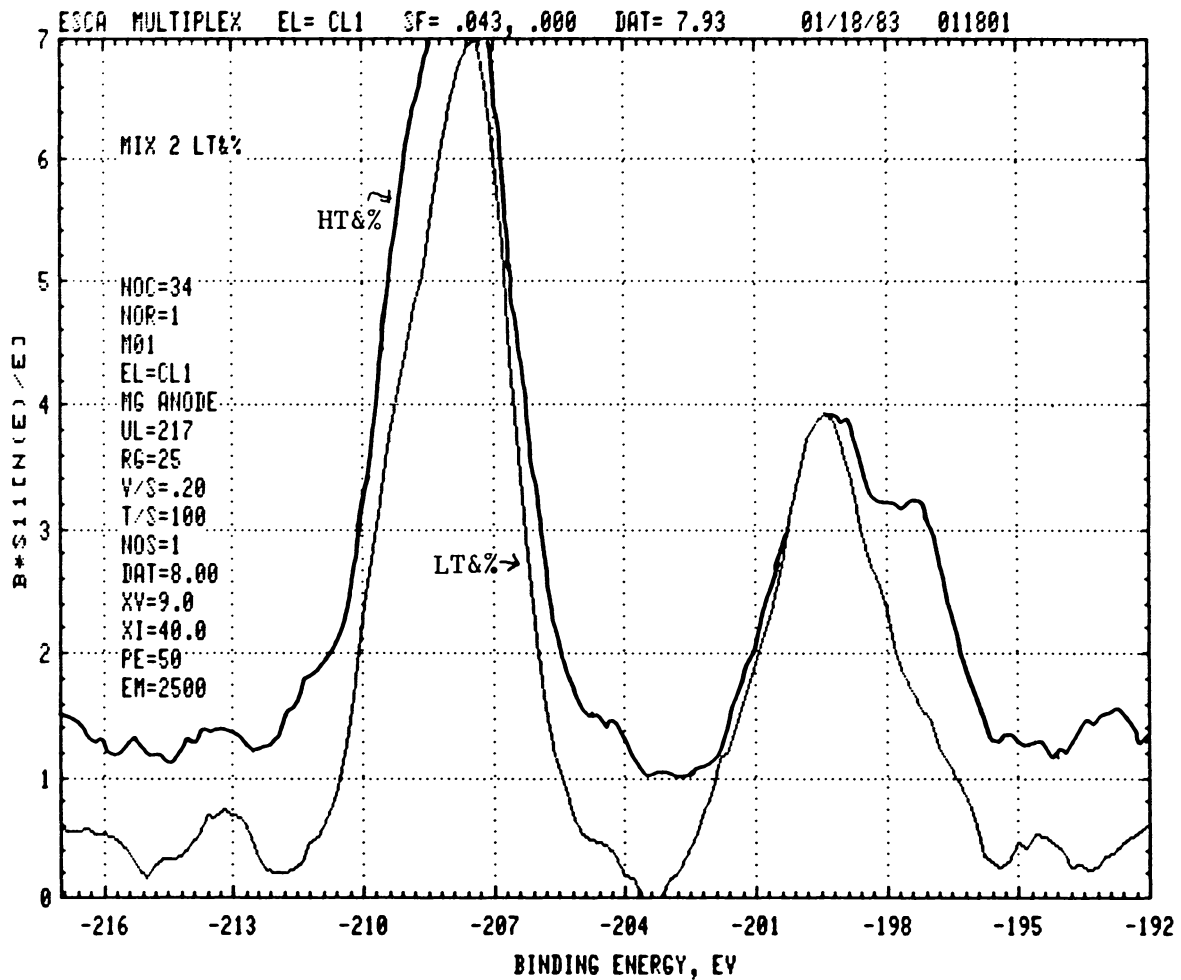


Figure 41. Cl^- Concentration Changes Between Mix 2 Ageing Conditions

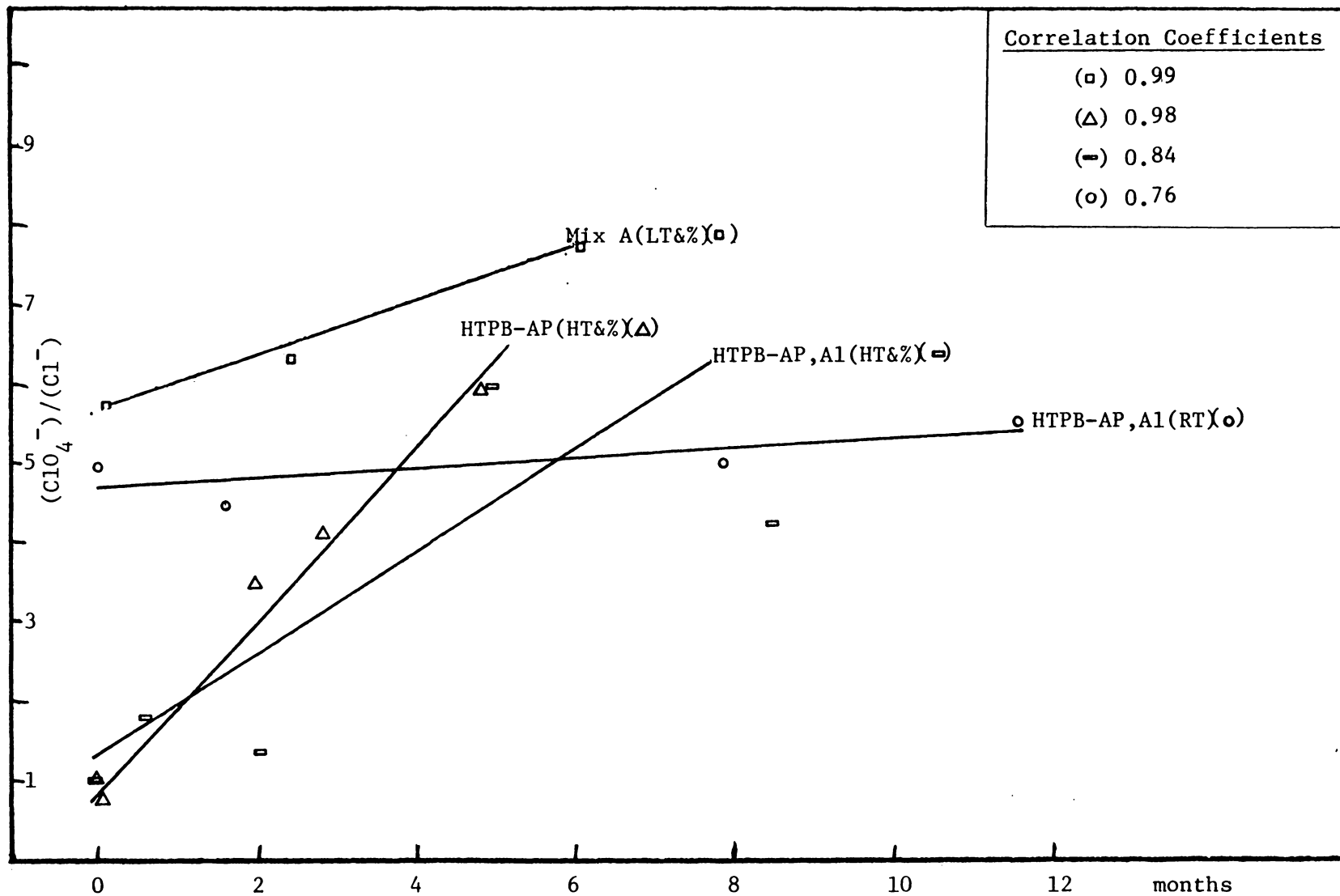


Figure 42. Longterm Cl⁻ Concentration Changes in Samples

rapidly. This might be due to NH_4Cl vapor pressure being such that it will preferentially sublime away at higher temperatures.

Summary

In summary, the XPS of propellant samples has shown that there is a loss of "organic" nitrogen as the propellant ages and that there is more NH_4Cl present in an aged vs unaged sample. Instrumental conditions leave doubt as to whether there is a consistent change in the AP/ NH_4Cl ratio over a period of time.

References

1. Pai Verneker, V. R., Kishore, K., and Mohan, V. K., AIAA Journal, 13(10), 1975, pp. 1415-1416.
2. Pai Verneker, V. R., Kishore, K., and Nair, M. N. R., AIAA paper #6191, Anaheim, CA, 1975.
3. Pai Verneker, V. R., Kishore, K., and Prasad, G., FUEL, 57, 1978, pp. 22-24.
4. Jacobs, P. W. M. and Russell-Jones, A., AIAA Journal, 5(4), 1967, pp. 829-830.
5. Jacobs, P. W. M. and Russell-Jones, A., Eleventh Symposium (International), Combustion, The Combustion Institute, Pittsburgh, PA, 1966, pp. 457-462.
6. Pittman, C. U., Jr., AIAA Journal, 7(2), 1969, pp. 328-334.
7. Pearson, G. S., and Hall, A. R., Oxidation and Combustion Reviews, 3, 1968, pp. 129-239.
8. Pearson, G. S., and Sutton, D., AIAA Journal, 4(5), 1966, pp. 954-956 also 5(2), 1967, pp. 344-346.
9. Osada, H., and Kakinouchi, N., Kogyo Kayaku Kyokaishi, 26, 1965, pp. 200-211.
10. Dauerman, L., Kimmel, H., and Wu, Y. J., Combust. Sci. and Technol., 5, 1972, pp. 129-133.
11. Verneker, V. R. P., Rajalekshmi, V. K., and Jain, S. R., Combust. Sci. and Technol., 17, 1977, pp. 99-104.
12. Schedlabauer, F., ICT Jahres., 1971, pp. 275-303 Chem. Abstr., 81(8), 1974, pp. 10855h.
13. Myers, G. E., Chem. Abstr., 83(10), 1975, pp. 82,249p.
14. Layton, L. H., paper presented at AIAA/SAE 11th Propulsion Conference, Anaheim, CA, September 29-October 1, 1975.
15. Kuletz, E., and Pakulak, J. M., Jr., Chem. Abstr., 60:10465a (1964).
16. Layton, L. H., Chem. Abstr., 79(16):94167r (1973).

17. Layton, L. H., Chem. Abstr., 83(26):195940u (1975).
18. Verneker, V. R. P., Kishore, K., and Prasad, G., Comb. and Flame, 36, 1979, pp. 79-85.
19. Verneker, V. R. P., Kishore, K., and Prasad, G., J. Appl. Polym. Sci., 24, 1979, pp. 589-593.
20. Kishore, K., Ravindran, K., and Sankaralingam, S., Comb. Sci. and Technol., 27, 1982, pp. 155-157.
21. Layton, L. H., Christiansen, A. G., and Carpenter, R. L., J. Spacecraft, 18(3), 1981, pp. 211-215.
22. Gray, C. A., and Hill, H. D. W., Industr. Res. Dev., March 1980, pp. 136-139.
23. Daskocilova, D., and Schneider, B., Pure & Appl. Chem., 54(3), 1982, pp. 575-584.
24. Mochel, V. D., J. of Polym. Sci.: Part A-1, 10, 1972, pp. 1009-1018.
25. Clague, A., van Broekhoven, J., and Glaauw, L. P., Macromol., May-June 1974, pp. 348-354.
26. Furukawa, J., et.al., J. of Polym. Sci., Polym. Letters, 11, 1973, 239-244.
27. Thomassin, J. M., et.al., J. of Polym. Sci., Polym. Letters, 11, pp. 229-232.
28. Mochel, V. D., et.al., J. of Polym. Sci., Polym. Letters, 11, 1973, pp. 453-455.
29. Gemmer, R. V., and Golub, M. A., Applic. of Polym. Spectr., 1978, Academic Press Inc., pp. 79-85.
30. Ku, Michael, M., M.S. Thesis, Virginia Polytechnic Institute and State University, 1977.
31. Lindsay, J. R., et.al., Appl. Spectr., 27(1), 1973, pp. 1-5.
32. Nefedov, V. I., et.al., Geokhimiya, No. 1, 1972, pp. 11-19.
33. Barrie, A., Chem. Phys. Lett., 19(1), 1973, pp. 109-113.
34. Prins, R., J. of Chem. Phys., 61(7), 1974, pp. 2580-2591.

35. Copperthwaite, R. G., and Lloyd, J., JESRP, 14, 1978, pp. 159-162.
36. Copperthwaite, R. G., and Lloyd, J., Nature, 271, 1978, pp. 141-142.
37. Copperthwaite, R. G., and Lloyd, J., J.C.S. Dalton, 1977, pp. 1117-1121.
38. Clark, D. T., and Dilks, A., J. Polym. Sci., Polym. Chem. Ed., 17, 1979, pp. 957-976.
39. Clark, D. T., and Thomas, H. R., J. Polym. Sci., Polym. Chem. Ed., 14, 1976, pp. 1671-1700.
40. Clark, D. T., and Thomas, H. R., J. Polym. Sci., Polym. Chem. Ed., 16, 1978, pp. 791-820.

**The vita has been removed from
the scanned document**

XPS and Carbon-13 NMR Spectroscopic Analysis of
Composite Rocket Propellants

by

E. Wayne Kauffman

(Abstract)

In this study the applicability of Carbon-13 NMR and XPS to the detection of chemical changes in a solid composite rocket propellant was studied. Storage at elevated temperatures was used to simulate the propellant ageing process. In the XPS analysis, changes in the sources for the N(1s) and Cl(2p) photopeaks were investigated. The propellant loses "organic" nitrogen as it ages. Changes in the amount of Cl⁻ present are in doubt due to instrumental considerations.

Carbon-13 NMR analysis showed that with increasing age of a sample there is a corresponding loss of vinylic groups from the binder. This loss of vinylic character is preferential in the order pendant >> cis > trans. Due to the long scan times involved this method is of limited utility for ageing analysis.